ATMOSPHERIC PROCESSING OF BROWN CARBON FROM OPEN BIOMASS BURNING

A Thesis
Presented to
The Academic Faculty

by

Haviland Forrister

In Partial Fulfillment
of the Requirements for the Degree
Master of Science in the
School of Earth and Atmospheric Sciences

Georgia Institute of Technology

August 2017

ATMOSPHERIC PROCESSING OF BROWN CARBON FROM OPEN BIOMASS BURNING

Approved by:

Dr. Rodney J. Weber, Primary Advisor
School of Earth and Atmospheric Sciences
Georgia Institution of Technology

Dr. Athanasios Nenes, Secondary Advisor
School of Earth and Atmospheric Sciences
School of Chemical and Biomolecular Engineering
Georgia Institution of Technology

Dr. Yuhang Wang
School of Earth and Atmospheric Sciences
Georgia Institution of Technology

Date approved: 25 July 2017

ACKNOWLEDGEMENTS

I would like to thank my primary advisor, Dr. Rodney Weber, for being the first professor at the college to show interest in me as a student, explaining the school practices, previewing various laboratories and groups to me, and offering me a place on his research team. He mentored me through my first stages of working with new software and accessing online data and served as a constant source of advice for any scientific questions I had. I am thankful for his honesty and support, which made me feel at home in the department. I am also thankful for the degree of freedom he gave me in regards to my research, once I began being externally funded.

I would like to thank my secondary advisor, Dr. Athanasios Nenes, for offering me a place in his group, which had various research interests and offered a backbone of support throughout any scientific difficulties. The group helped me become a better presenter of science and a better-rounded atmospheric scientist. I am also thankful for the scientific insights Dr. Nenes provided in both grant applications and research presentations. From Dr. Nenes' research group, I would like to express appreciation particularly for the advice and knowledge imparted to me by James Hite, Jack Lin, and Sara Purdue. They made me feel welcome in the group, helped me with presentations of my research and reviews of scientific principles, and ultimately ended up contributing in small part to the development of this thesis. I would not have gotten as far without their humor and support.

Finally, I would like to acknowledge Dr. Yuhang Wang, who came in later to my research with a shared post-doctorate student, Dr. Yuzhong Zhang, who approached my data using a modeling perspective and helped to strengthen my modeling capabilities. The group

meetings shared with all four professors helped to increase my knowledge about the field of atmospheric science as a whole and to help focus my thesis study.

I would also like to acknowledge the support provided to me by my former research and laboratory supervisors: Dr. Chris DePree, Dr. Peter Chen, and Dr. Gary Gimmestad. Throughout my graduate career, these three individuals kept touch with my progress, my research and career interests, and my personal happiness. I could not be more happy or thankful for these threads that I have managed to stay connected to, whose emotional and career support I never question. They always had time to lend an ear to my troubles and provide avenues for me to stay involved with old colleges and students with whom I had worked.

TABLE OF CONTENTS

LIST OF TABLES

LIST OF FIGURES

LIST OF SYMBOLS AND ABBREVIATIONS

SYMBOLS

AAE	Absorption Ångström Exponent, unitless
AAE_{BrC}	Absorption Ångström Exponent for brown carbon
$b_{ap}(\lambda)$	Bulk aerosol light absorption coefficient, at specified wavelength
ρ	Particle density, g/cm^3

ABBREVIATIONS

AMS	Aerosol Mass Spectrometer
BC	Black Carbon
BrC	Brown Carbon
CO	Carbon monoxide
DC3	Deep Convective Clouds and Chemistry
MAC	Mass Absorption Cross-section
OA	Organic Aerosol
PSAP	Particle Soot Absorption Photometer
RF	Radiative Forcing
SBDART	Santa Barbara DISORT Atmospheric Radiative Transfer
SEAC4RS	Studies of Emissions, Atmospheric Composition, Clouds, and Climate Coupling by Regional Surveys
SP2	Humidified Dual Single Particle Soot Photometer
TOA	Top of the atmosphere

SUMMARY

Brown carbon (BrC) refers to the light-absorbing portion of organic aerosol (OA), which is primarily emitted from biomass burning and fossil fuels and secondarily formed through various means. BrC has been found to be ubiquitous in the atmosphere and, from what measurements exist, has been predicted to have important effects on radiative forcing [*Liu et al*., 2014, 2015]. However, the lifecycle and atmospheric stability of BrC from biomass burning are virtually unknown. Laboratory experiments of secondary BrC suggest it may photobleach in the atmosphere [*Lee et al.*, 2014; *Zhao et al.*, 2015] and have aging mechanisms not shared with organic aerosol or black carbon (BC), which are also emitted from biomass burning and have important radiative forcing effects.

As presented in Chapter 2, measurements of BrC aerosol light absorption taken from intense wildfire plumes transported over two days, during the 2013 NASA SEAC4RS mission, are seen to evolve over time. Concurrent measurements of OA and BC mass concentration, BC coating thickness, absorption Ångström exponent (AAE), and OA oxidation state (O/C) reveal that BrC initially emitted from the fires was largely unstable. Using back trajectories to estimate the transport time, BrC aerosol light absorption was found to decay in the plumes with a half-life of 9 to 15 hours, measured over day and night. Although most BrC was lost within a day, possibly through photobleaching, chemical loss, and/or evaporation, the remaining persistent fraction likely determines the background BrC levels most relevant for climate forcing. While large coefficient of determinations exist between BrC, AAE, O/C, and f60 for these single-fire measurements, later multiple-fire measurements show that BrC is only consistently correlated

with bulk aerosol AAE. This correlation is non-linear, however, so bulk aerosol AAE cannot be used to predict BrC light absorption.

Current models of BrC use static primary emission characteristics to predict BrC radiative forcing effects, primarily employing a correlation between k_{OA} (the imaginary part of the refractive index of OA) and the ratio of BC/OA for a source fire. Considering the dissipation of BrC over the course of 10 hours due to photobleaching, this relatively simple model of predicting BrC absorption post-emission from biomass burning may be overestimating the contribution of BrC to absorbing aerosol radiative forcing. In Chapter 3, using BrC spectrophotometric data taken aboard NASA's 2012 DC3 and 2013 SEAC4RS campaigns, the changing optical properties of BrC—both its direct absorption and its wavelength dependence—and vertical distribution of BrC in the atmosphere combine to cause potentially significant errors in radiative forcing when k_{OA} is predicted by BC/OA. Both show significant differences between actual measurements and predicted values outside of biomass burning plumes in the background aerosol, while the interior of plumes seems to be relatively well described by a BC/OA parameterization of k_{OA}. Ultimately, it is found that capturing the enhancement of BrC with altitude is more important to radiative forcing models than capturing the BrC optical aging mechanisms, at least for measurements over the continental United States. Discussions on future research questions related to the non-global nature of these studies, and possible reasoning behind the vertical profile, are presented in the concluding remarks.

CHAPTER 1

INTRODUCTION

1.1 Motivation for Studying Brown Carbon

"Aerosol" is the term for solid and liquid particulate matter floating in a gaseous medium, which exists everywhere in the atmosphere. The most important atmospheric aerosols include: inorganic compounds, organic compounds (often termed organic aerosol, or OA), black carbon (emitted from incomplete combustion of fossil fuels and biomass), and mineral dust [*Boucher et al.*, 2013]. The prevalence of each aerosol fluctuates depending on the region. All aerosols interact with sunlight, whether incident or reflected, causing a positive or negative amount of radiative forcing that affects climate. There are two main methods of aerosols affecting radiative forcing, termed direct and indirect forcing. Direct radiative forcing is caused by aerosols directly absorbing or scattering sunlight, causing warming or cooling of the atmosphere [*Haywood and Shine*, 1995; *Forster et al*., 2007]. Indirect radiative forcing is caused by the interaction of aerosols with clouds, whereby aerosols act as cloud condensation nuclei and alter the microphysical properties of clouds, affecting cloud reflectivity and lifetime [*Kaufman et al*., 2005; *Forster et al*., 2007]. Semi-direct effects are those where absorbing aerosols disturb the altitude profile of temperature, which affects static stability of the atmosphere and localized weather phenomena. In addition to radiative forcing, aerosols that absorb light in the ultraviolet spectrum decrease concentrations of photochemical smog, especially tropospheric ozone [*R.R. Dickerson et al.*, 1997; *He and Carmichael*, 1999], which is hazardous to health [e.g., *U.S. EPA*, 2013]. Therefore, understanding the absorptive properties of various aerosols is imperative to

accurately predicting absorbing aerosol radiative forcing, ascertaining absorbing aerosols' total effect on climate, and determining their effect on health.

The main light-absorbing aerosols are black carbon (BC) and mineral dust [*Boucher et al.*, 2013]. BC dominates light-absorption in most regions of the world due to its strong wavelength-independent absorptivity ($k_{BC} \approx 0.79$ for 550nm), which designates equal strength in both radiative forcing relevant wavelengths and photochemically relevant wavelengths [*Bond and Bergstrom*, 2006; *Bond et al.*, 2013]. BC absorption can be enhanced due to internal mixing with dust or OA; the mixed material is often assumed to form a shell around a core of BC [*Lack et al.*, 2010; *Saleh et al.*, 2013]. A subset of OA molecules, which typically scatter light, has recently been found to absorb strongly in the near-ultraviolet wavelengths and weakly in the short visible wavelengths. This subset is collectively called brown carbon (BrC) due to its yellow-brown coloring [*Andreae and Gelencser*, 2006; *Laskin et al.*, 2015]. Because of the multitude of chromophores comprising BrC, its optical properties and absorption characteristics are still poorly understood in literature, with wavelength-dependent absorptivities for fresh emissions ranging across several orders of magnitude ($k_{OA} \approx 0.003\text{-}0.22$) [*Saleh et al.*, 2014].

Biomass burning is a major global source of both BC and OA [*Bond et al*., 2004], with significant effects on radiative forcing, climate, and health. Similarly to BrC, some mineral dust also absorbs light in the ultraviolet and visible wavelengths, especially ferric iron oxides (e.g., hematite, goethite) [*Sokolik and Toon*, 1999]. Asian dust is continuously present in background aerosol on the western U.S. coast [*Duce*, 1995; *Perry et al*., 2004] and likely accounts for some fraction of radiative forcing in this region. Absorption properties for all aerosols are highly dependent on their mixing state with other aerosols, where external mixing allows for the absorbing aerosols to retain their typical optical properties while internal mixing enhances these

properties [*Bergstrom et al*., 2004; *Bond and Bergstrom*, 2006; *Schnaiter et al.*, 2005]. This complicates interpretations of absorption measurements for aerosol mixtures.

The degree to which each of these aerosols absorb light, their concentrations in the atmosphere, their mixing state with other aerosols, and their altitude profiles are all important factors that affect radiative forcing over a region. Atmospheric measurements of each are, therefore, essential to effectively determining global radiative forcing caused by absorbing aerosols. However, no airborne or ground measurement campaign to date has managed to measure all classes of light-absorbing aerosols independently. Instead, bulk aerosol light-absorption and light-scattering measurements are typically conducted, and the relative abundances and optical properties of each aerosol are then estimated from these bulk measurements. With decreasing degrees of confidence, this can be achieved using aerosol size distributions to separate biomass burning aerosols from dust [e.g., *Petzold et al*., 2011], retrieved optical properties like absorptivities [*Schuster et al*., 2016a], and inferences from the wavelength dependence of bulk aerosol absorption [*Schuster et al.*, 2016b]. Nevertheless, separating the bulk aerosol absorption into its various species is essential to constraining aerosol forcing uncertainties [*Forster et al.*, 2007] and improving emission-based control policies. Detailed investigations into the chemical composition and optical properties of absorbing aerosols is vital to determining their impact on climate.

In the NASA DC-8 research aircraft campaigns in the summers of 2012 and 2013, respectively termed DC3 (Deep Convective Clouds & Chemistry) and SEAC4RS (Studies of Emissions, Atmospheric Composition, Clouds and Climate Coupling by Regional Surveys), aerosol light-absorption measurements were made for bulk aerosol and specifically for BrC. BC and OA mass concentrations were also measured. For this campaign, a determination of both

atmospheric BrC and bulk aerosol light-absorption for a range of altitudes (from near-surface to 13 km) and regions (from western to southeastern U.S.) was made possible.

This thesis aims to understand BrC from emission to its aged and background levels with specific focus on its aging mechanisms post-emission, vertical profile, and optical properties. Previous BrC studies have primarily been laboratory measurements of biomass combustion, with few atmospheric BrC measurements being made. Of the available atmospheric BrC measurements, few were obtained by direct means. The data set to be discussed is the first of its kind: direct BrC measurements at a range of altitudes from a variety of locations in the United States. The opportunity provided by the data set for studying the aforementioned properties of BrC is novel. The scientific objectives of this thesis focus on how BrC primarily emitted from open biomass burning (including wildfires and agricultural fires) optically ages in the atmosphere and contributes to background aerosol levels present from the boundary layer to the top of the atmosphere. Relationships will be drawn between BrC, BC, OA, chemical properties of the OA, and the wavelength dependence of bulk aerosol light-absorption (AAE).

1.2 Sources and Importance of Brown Carbon

BrC consists of a myriad of mostly unidentified organic compounds with primary and secondary formation mechanisms. It is unknown whether the observed BrC absorption spectra arises due to isolated molecular compounds or supramolecular aggregates, or whether BrC is composed of scant few strong chromophores or mixtures of weak chromophores [*Laskin et al.*, 2015]. Primary formation occurs during incomplete combustion of biomass [*Andreae and Gelencser*, 2006; *Hoffer et al*., 2006; *Chakrabarty et al*., 2010; *Chen and Bond*, 2010; *Hecobian et al.*, 2010; *Kirchstetter and Thatcher*, 2012; *Lack et al*., 2013; *Saleh et al*., 2013, 2014] and fossil fuels [*Bond*, 2001; *Yang et al*., 2009; *Hecobian et al.*, 2010; *Zhang et al*., 2011, 2013].

Two major components of BrC have been identified for primary emissions: humic-like substances (HULIS) [*Graber and Rudich*, 2006; *Hoffer et al.*, 2006] and nitroaromatics [*Iinuma et al*., 2010; *Kitanovski et al.*, 2012; *Desyaterik et al*., 2013; *Zhang et al*., 2013]. Biomass burning BrC measured on filters suggests that BrC contains highly polar molecules, less polar molecules, water-soluble components, and insoluble components [*Chen and Bond*, 2010]. Water-insoluble components show greater absorption per mass than water-soluble components and are likely due to high-molecular weight polycyclic aromatic hydrocarbons [*Chen and Bond*, 2010].

Secondary BrC formation has been inferred from atmospheric measurements of vehicle emissions [*Zhang et al.*, 2011, 2013] and laboratory measurements of photochemically aged biomass burning [*Saleh et al*., 2013]. Various laboratory experiments have also formed BrC-like chromophores using photooxidation of aromatics [*Lambe et al*., 2012]; ozonolysis of terpenes [*Bones et al*., 2010; *Nguyen et al*., 2012; *Laskin et al.*, 2014]; and aqueous phase reactions of lignin and isoprene oxidation [*Limbeck et al*., 2003; *Hoffer et al.*, 2006], reactions of carbonyls with amines [*De Haan et al*., 2009; *Zarzana et al*., 2012], and reactions of carbonyls with ammonium salts [*Shapiro et al.*, 2009; *Sareen et al*., 2010; *Lin et al*., 2015]. Chemical speciation of these studies have found that secondary BrC absorption is likely due to nitroaromatics, reduced-nitrogen organic compounds [*Lin et al*., 2015], and other high-molecular weight compounds produced in the atmosphere by reactions between carbonyls and ammonia/amines [*Shapiro et al.*, 2009; *Sareen et al*., 2010]. Charge-transfer interactions between chromophores in colored dissolved organic matter may also lead to these absorption characteristics.

When sensitive direct measurement techniques—such as light absorption of aerosol extracts—are used, BrC is found to be ubiquitous, present even in the remote continental

troposphere at 10 km altitude [*Kieber et al.*, 2006; *Hecobian et al.*, 2010; *Liu et al., 2014*, 2015]. Recent studies suggest that aerosol components from biomass burning are more prevalent than previously thought [*Hennigan et al.*, 2010; *Hennigan et al.*, 2011; *Bougiatioti et al.*, 2014], and may strongly contribute to this observed background BrC [*Washenfelder et al.*, 2015]. Further, light absorption by BrC may globally offset the total climate cooling at the top of the atmosphere from direct radiative forcing of OA [*Feng et al.*, 2013]. Vertical profiles of BrC measured *in-situ* confirm its importance, as it can account for 20% of the aerosol direct radiative forcing at the top of the atmosphere [*Liu et al.*, 2014].

1.3 Radiative Forcing of Brown Carbon

Direct radiative forcing involves the absorption or scattering of solar radiation by aerosols. BC is the most absorbing aerosol in the visible wavelengths [*Bond et al*., 2013], which are sensitive to light-absorption due to the lack of atmospheric absorbers in this region. BC is primarily emitted in large quantities from fossil fuel combustion and biomass burning. BC has been found to have significant effects on radiative forcing and, thus, warming of the climate. Meanwhile, OA—which is also primarily emitted from fossil fuel and biomass combustion—has been considered to typically scatter incoming solar radiation, with a net cooling effect on climate. In total, open biomass burning accounts for 33% of the global BC burden and 66% of the global primary organic aerosol burden, indicating that it is an important source of climate forcing, both positive and negative [*Bond et al.*, 2004]. Although fossil fuel controls are working to reduce BC and OA primary emissions, open biomass burning (like wildfires) is largely caused by natural factors, cannot be effectively controlled, and is likely to increase in response to climate change. Due to temperature increases caused by our changing climate, primary BC and OA emissions are expected to enhance by roughly 20% (for BC) and 40% (for organic carbon) in

the next several decades, predominantly caused by increased wildfire emissions [*Spraklen et al.,* 2007]. Therefore, understanding the radiative forcing effects of BC and OA, resulting from biomass burning, is imperative for future climate studies.

Radiative forcing models for light-absorbing aerosols (typically only BC) have large discrepancies between the observationally-constrained and emissions-based approaches, with a range of 0.1 to 1.63 W m^{-2} [*Bond et al.,* 2013]. This discrepancy is likely due, in part, to the treatment of OA as purely scattering and the lack of internal mixing considerations of BC with other aerosols [*Saleh et al.,* 2015]. Aerosol models that simulate microphysical processes suggest that BC can become internally mixed with other material in 1-5 days [*Jacobson*, 2001] and be transported to all altitudes [*Aquila et al.,* 2011]. When BrC is simulated as externally mixed with BC in radiative forcing models, BrC is found to contribute +0.1 – +0.57 W m^{-2}, or between 25-70% of the forcing due to BC [*Feng et al.,* 2013; *Lin et al.,* 2014], and roughly 15% of the forcing by total absorbing aerosols [*Park et al.,* 2010]. In contrast, a recent model simulating both external and internal mixtures of BrC with BC showed +0.22 W m^{-2} for externally mixed BrC and +0.12 W m^{-2} for internally mixed BrC [*Saleh et al.,* 2015]. The latter study also found that including both lensing and BrC absorption in models increased the direct radiative effect for biomass combustion aerosols from negative (cooling) to positive (warming), helping reduce the gap between the observationally-constrained and emissions-based radiative forcing model results. In order to calculate both the internal and external mixing of BrC, *Saleh et al.* [2015] made use of their parameterization determined from laboratory biomass combustion experiments, where k_{OA} and the wavelength dependence of k_{OA} were found to correlate highly with the ratio of BC/OA [*Saleh et al.,* 2014]. Previous radiative forcing models used a fixed

mass absorption cross-section (MAC) for BrC [*Park et al.*, 2010] or two values of k_{OA}, as upper and lower limits of BrC absorption [*Feng et al.*, 2013], in order to estimate BrC radiative forcing.

The difficulties with the previous modeling approaches center around an assumption of the optical constancy of BrC post-emission. Laboratory experiments seem to suggest that BrC may photochemically change over time, with BrC bleaching when continually exposed to light [*Zhong and Jang*, 2014; *Lee et al.*, 2014; *Zhao et al.*, 2015] with half-lives of a few minutes to a few hours. This phenomenon has not previously been studied in the atmosphere, so it is unknown the scale to which this could affect BrC parameterizations in atmospheric models of biomass burning. Other aging mechanisms of BrC post-emission are also unknown, making the assumption that their optical properties remain stable over time quite tenuous. These issues will be the primary focus of this thesis (Chapter 2). Furthermore, if a method requires predicting BrC from other species like BC and OA, then it would be important to ascertain the degree to which BrC behavior follows BC and OA in a biomass burning plume. How these changes might affect radiative forcing predictions of BrC will be the secondary focus of this thesis (Chapter 3).

CHAPTER 2

EVOLUTION OF BROWN CARBON IN OPEN BIOMASS BURNING PLUMES

2.1 Introduction

As controls continue to reduce fossil fuel emissions and a changing climate potentially leads to more fires, both the relative and total impact of biomass burning on air quality and climate forcing is expected to increase [*Fuzzi et al., 2015*]. Although studies have focused on a ratio of BC to OA in emissions of relatively briefly aged biomass burning to predict BrC in large scale radiative forcing modeling endeavors [*Saleh et al.*, 2014], there is a growing body of evidence that atmospheric BrC evolves differently from both BC and bulk OA, owing to production of BrC from secondary organic aerosol and loss of BrC from photobleaching [*Lee et al.*, 2014; *Zhong and Jang*, 2014; *Zhao et al.*, 2015], volatilization, or aerosol-phase reactions. In order to understand the difference between BrC and bulk OA evolution and determine BrC climate effects, a focused effort to measure its atmospheric distribution and evolution is needed.

In this chapter, the evolution of BrC is charted using airborne data from two large wildfire plumes sampled from near-emission to over two days of atmospheric transport. This study constitutes the first reported evolution of BrC from biomass burning in the atmosphere.

2.2 Method

In situ measurements were conducted onboard the NASA DC-8 airborne platform as part of the SEAC4RS mission. Sampling occurred from 6 August to 23 September 2013 over the western, central, and southeastern regions of the continental US. SEAC4RS followed the DC3 campaign, where the DC8 flew with the same instrument payload.

BrC spectrophotometric measurements were made for liquid extracts of aerosols collected on filters. Aerosols with aerodynamic diameter less than 4.1 μm were collected on Teflon (EMD Millipore) filters on the aircraft over roughly 5 to 10 minutes and then stored at -10°C. The filters were extracted in water and then methanol to select for water-soluble BrC and water-insoluble BrC, respectively. BrC absorption spectra were obtained over 200-800 nm using a 2.5-m path-length Liquid Waveguide Capillary Cell attached to a ultraviolet-visible spectrophotometer. The technique of removing insoluble components from filters after water extracts allows for direct BrC absorption measurements, in contrast to other methods measuring total aerosol absorption and estimating BrC absorption. BrC absorption is reported for the total BrC (water-soluble plus water-insoluble), which accounts for almost all biomass burning BrC. A small percentage may not be soluble by either methanol or water, but this portion likely has low absorption [*Chen and Bond*, 2010]. For the rest of Chapter 2, "BrC" will refer to the average light-absorption of the dissolved aerosol in the solvent between 360 and 370 nm (in Mm^{-1}). This wavelength region accentuates the portion of BrC important to photochemistry and ozone reduction, is consistent with former studies [*Hecobian et al*., 2010; *Zhang et al*., 2011, 2013; *Liu et al*., 2014, 2015], and avoids contribution by non-organics (like nitrate).

Bulk aerosol light absorption coefficients ($b_{ap(\lambda)}$) at three wavelengths (470, 532, 660nm) were measured with a Particle Soot Absorption Photometer (PSAP) for aerosols below 4.1 μm aerodynamic diameter and were corrected for artifacts associated with filter-based optical absorption measurements as described by *Virkkula et al.* [2010]. Absorption Ångström exponents were determined from the 470 and 532 nm wavelength pair by:

$$AAE_{PSAP} = - \frac{\ln\left(b_{ap,PSAP}(532)\right) - \ln\left(b_{ap,PSAP}(470)\right)}{\ln(532) - \ln(470)} \quad (2.1)$$

Particle chemical composition was determined with a High Resolution Time of Flight Aerosol Mass Spectrometer (AMS) [*DeCarlo et al.*, 2006] that measured bulk aerosol particles nominally below 1 μm aerodynamic diameter. Here, we use the overall OA concentrations and the O/C (oxygenation) [*Aiken et al*., 2008]. O/C was determined using the organic mass fraction of the AMS data using the updated calibrations of *Canagaratna et al.* [2015]. The mass ratio of biomass burning tracer signal (arising from levoglucosan and related molecules) to OA, f_{60}, was calculated from the AMS data by taking the ratio of the signal at *m/z* 60 to the total organic mass signal [*Cubison et al.*, 2011]. Refractory black carbon (BC) mass concentrations were determined with a SP2 (Single Particle Soot Photometer) and were corrected for particle sizes outside the measurement range [*Schwarz et al*., 2008]. SP2 data were also used to estimate BC coating thickness for dried aerosol sampled in the individual plumes using the methodology of *Schwarz et al.* [2008] for particles with 3 to 5 fg refractory BC mass content. The dry modal coating thickness was reported every 5 to 10 min. Carbon monoxide (CO) was measured as a mixing ratio using Diode laser spectrometry to make a Differential Absorption CO Measurement at 1 s intervals [*Sachse et al*., 1987].

In the analysis, BrC was first plotted against the CO concentration to identify which filter sampling periods corresponded to the most intense regions of the plume and to exclude filters with a significant sample integration period not associated with the plume. For each aircraft transit through a plume, BrC data from the filters were selected based on filter sample integration times corresponding to the most significant CO enhancements within the plume (CO "peaks"). If more than one filter sample existed within a given "peak," the data were averaged over those filter sampling times. Once the in-plume filters were identified, all parameters of interest were merged to the filter sampling times if the data covered was greater than 75% of the filter

integration time; this merged data was retrieved from the NASA SEAC4RS archive (the 19 May 2014 merge), except for the HR-ToF-AMS data that were updated 24 Oct. 2014. Aerosol data are reported at standard temperature and pressure (1 atm, 273.15 K).

To account for dilution with plume transport, Normalized Excess Mixing Ratios (NEMRs) [*Hobbs et al*., 2003] were calculated using CO as the conservative tracer (e.g., $\Delta X/\Delta CO$). Background concentrations for the various NEMRs and CO were determined from data averaged before and after each plume intercept. NEMRs were generated for BrC, BC, and OA. Intensive parameters, including the AAE, BC coating thickness, O/C, and f60, are not presented as NEMRs. Air mass transport times, in hours since emission, were used as the metric for degree of plume evolution based on HYSPLIT back trajectories from the point of aircraft measurement to the fire source location. The fire source latitude and longitude were retrieved from INCIWEB reports (*http://inciweb.nwcg.gov/*) for the Rim and Elk Complex Fires, described below. For each plume measurement, the amount of time the air mass was exposed to sunlight during transport from the fire to the point of measurement was also estimated in order to investigate possible photochemical effects on BrC evolution. HYSPLIT back trajectories verified that the various plume intercepts analyzed were from a common fire, or region of fires given the limited degree of spatial resolution available by this method.

2.3 Results

2.3.1 The Rim Fires

Although many plumes from both agricultural and wildfires were intercepted during SEAC4RS, here we focus on the Rim fires (named due to their proximity to the scenic point "Rim of the World" in California) since these were the largest plumes detected, and hence most amenable to aerosol analyses via filters. The Rim fires produced smoke plumes studied over two

consecutive days. On the first day, 26 Aug. 2013, the aircraft investigated the smoke downwind from an extensive fire near Yosemite National Park, California, referred to as the Rim 1 fire. HYSPLIT trajectories tracked the smoke as it moved northeast through Nevada, Oregon and Idaho, where other regional fires were mostly avoided by the aircraft (Figure 2.1). On 27 Aug. 2013, the goal was to pick up this plume and continue to track it. However, the Rim 1 plume passed over another active burning region in Idaho, the Elk Creek Complex fire, and then moved from Idaho, through Montana, and into Manitoba, Canada (Figure 2.1). The plume from this second day is referred to as Rim 2, since delineating the smoke from the Yosemite and Elk Creek Complex fires via HYSPLIT trajectories is not clear-cut. In the following, we analyze the BrC evolution both by: 1) assuming all smoke is from the Yosemite fire; and 2) assuming that the primary smoke sampled during the Rim 2 flight was from the Elk Creek Complex fire. This

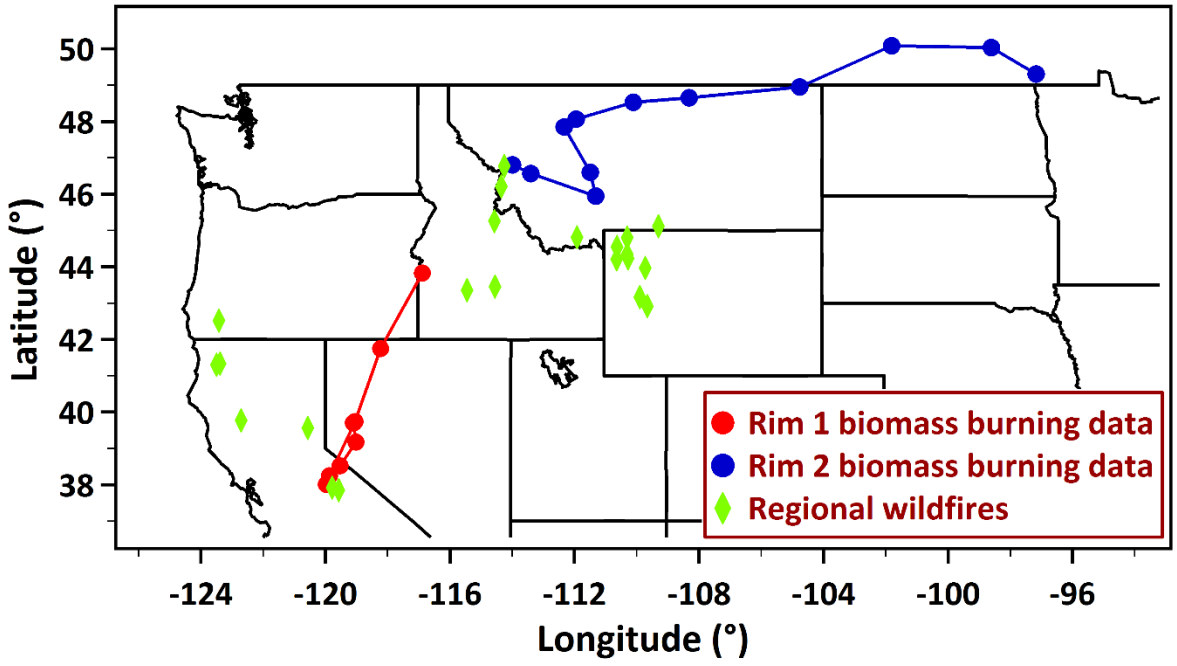

Figure 2.1: Map of the SEAC4RS flight trajectory for 26 and 27 August 2013.

provides a discrete range in BrC evolution times. Other parameters of interest are plotted assuming the Rim 2 smoke is solely from the Elk Creek Complex fire, for simplicity. The Rim 1 data tracks from about 1 to 7 hours of plume age, while the Rim 2 data tracks from 9 to 50 hours if the source is assumed to be the Elk Creek Complex fire (or 17 to 40 hours, assuming the Yosemite fire). The combined Rim 1 and 2 data provide an opportunity to study the evolution of BrC and other aerosol properties for over two days of transport, corresponding to a transport distance of 1500 km.

2.3.2 Measurements in Smoke Plume

For the two Rim flights, the plumes are easily identified close to the fires by high correlations between BrC and CO concentrations (for both flights combined, BrC and CO were correlated with $r^2 = 0.98$), indicating BrC enhancements are associated with smoke plumes (Figure 2.2).

To test our analysis method, given uncertainty imposed by the filter sampling times and

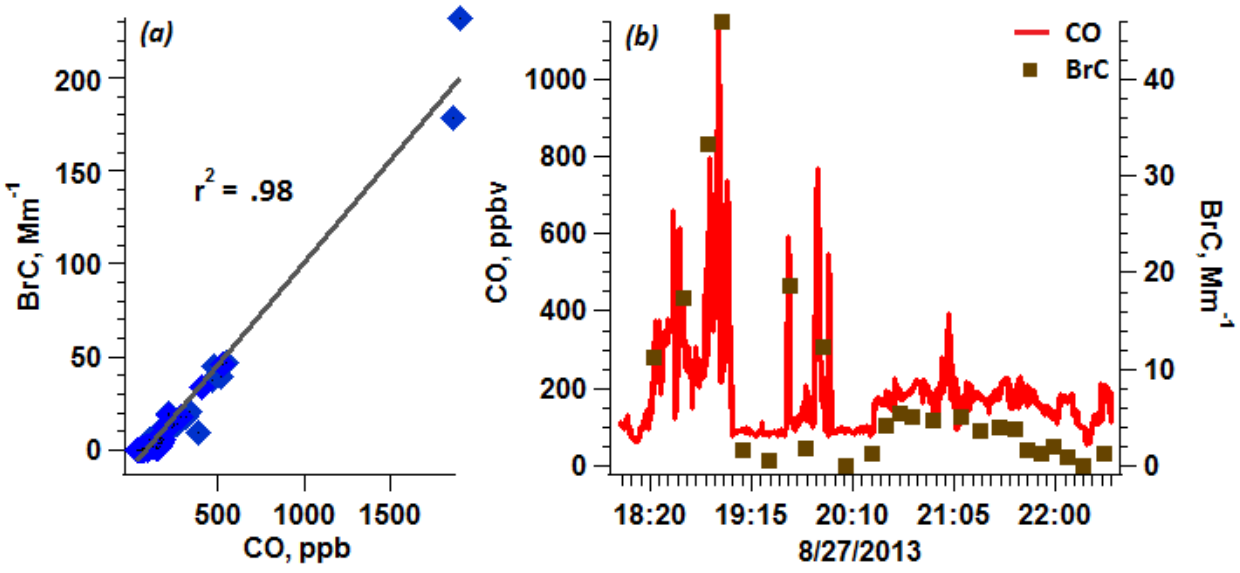

Figure 2.2: BrC and CO are highly correlated in fires and background air.

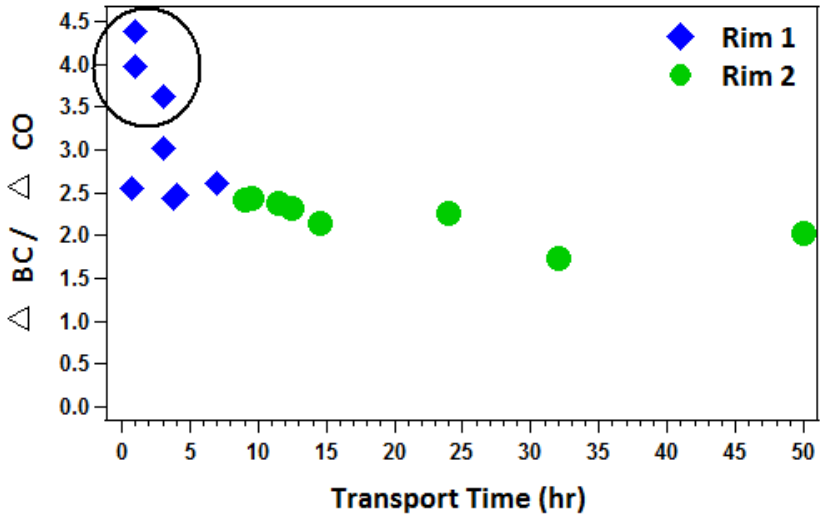

Figure 2.3: Black carbon evolution in Rim smoke plumes, assuming Elk Creek Complex fire for Rim 2.

plume widths, we first plot the NEMR for BC for both Rim 1 and Rim 2 smoke plumes (Figure 2.3), assuming Rim 2 data resulted from the Elk Creek Complex fire. CO and BC are both emitted from biomass burning and should both be approximately conserved in transport in the free troposphere in the absence of precipitation over these timescales. Thus little change is expected with plume age, as is seen. At the beginning of both the Rim 1 and Rim 2 fires, there was scatter in the ΔBC/ΔCO (the circle in Figure 2.3), which appear to result from smoke plumes from separate local fires having different BC relative to CO emissions. All data corresponding to these times are excluded from the overall plume evolution for the following analysis.

Figure 2.4 shows the evolution of BrC concentration (via proxy solution extract light absorption at 365 nm), where the transport time was calculated assuming Rim 2 originated from both the Elk Creek Complex and the Yosemite fires. In contrast to ΔBC/ΔCO, which was relatively constant over time, BrC in these plumes decreased over transport with an approximate half-life of 9 hours, assuming the Elk Creek Complex fire, or 15 hours, assuming the Yosemite

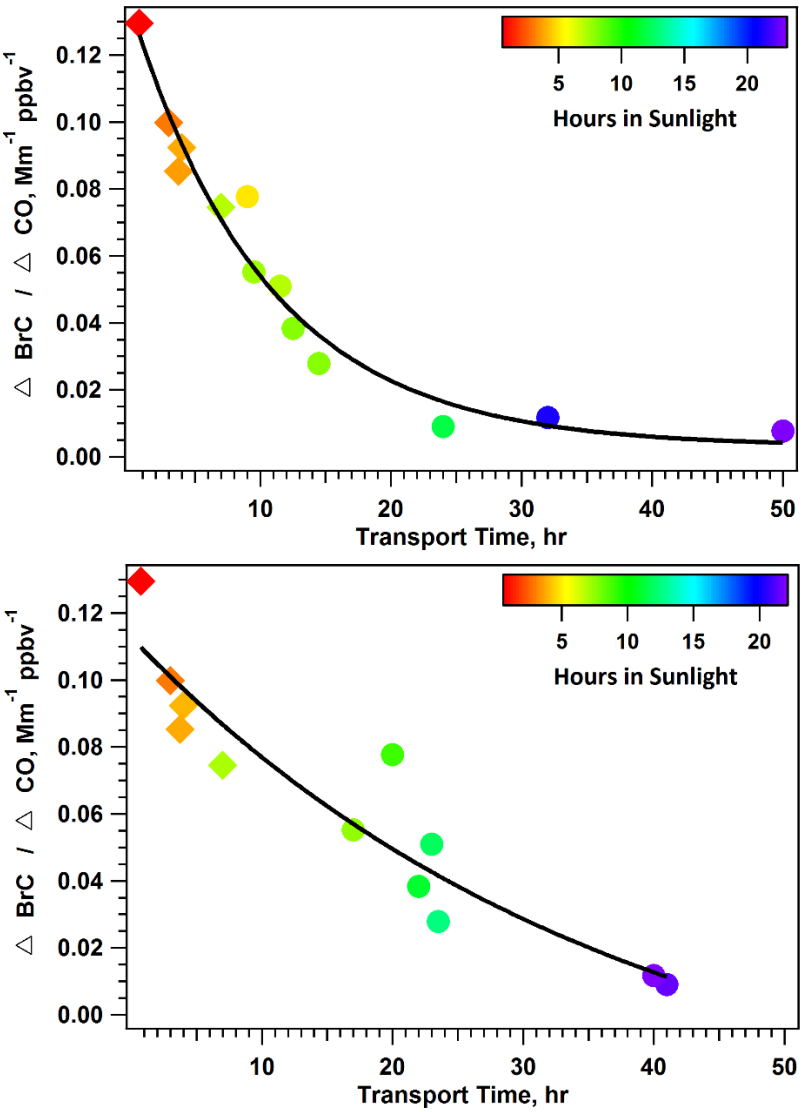

Figure 2.4: BrC evolution in the Rim smoke plumes; exponential fit shows the loss of BrC. Diamond indicates Rim 1; circle indicates Rim 2. Color shows smoke plume sunlight exposure during transport. Rim 2 transport times assume separate sources: (a) for Elk Creek Complex fire and (b) for Yosemite fire.

fire as the source of Rim 2 smoke. If any mixing of the smoke from the two fires occurred, the half-life should fall between these two extremes. The color scale on Figure 2.4 represents the approximate amount of sunlight that the sampled smoke aerosol was exposed to. With increased sun exposure, the BrC continued to decrease. However, after about 12 hours, continued sun exposure showed no effect; it is likely all the chromophores that could be affected by

photochemistry or photobleaching were eliminated by this time. This result is consistent with laboratory experiments showing BrC photobleaching [*Lee et al.*, 2014; *Zhong and Jang*, 2014; *Zhao et al.*, 2015], although the photobleaching experiments found much shorter half-lives of a few minutes to hours and do not consider the solar cycle. Reduced light absorption with time suggests a BrC loss mechanism such as chemical bleaching (chemical reactions resulting in the destruction of the chromophores). Evaporation (or volatilization) may also be occurring.

As expected if BrC is being bleached or removed, the net aerosol AAE should decrease with age, as can be seen in Figure 2.5a, where AAEs of 3.5 to 4.0 near the fire drop toward 1 at

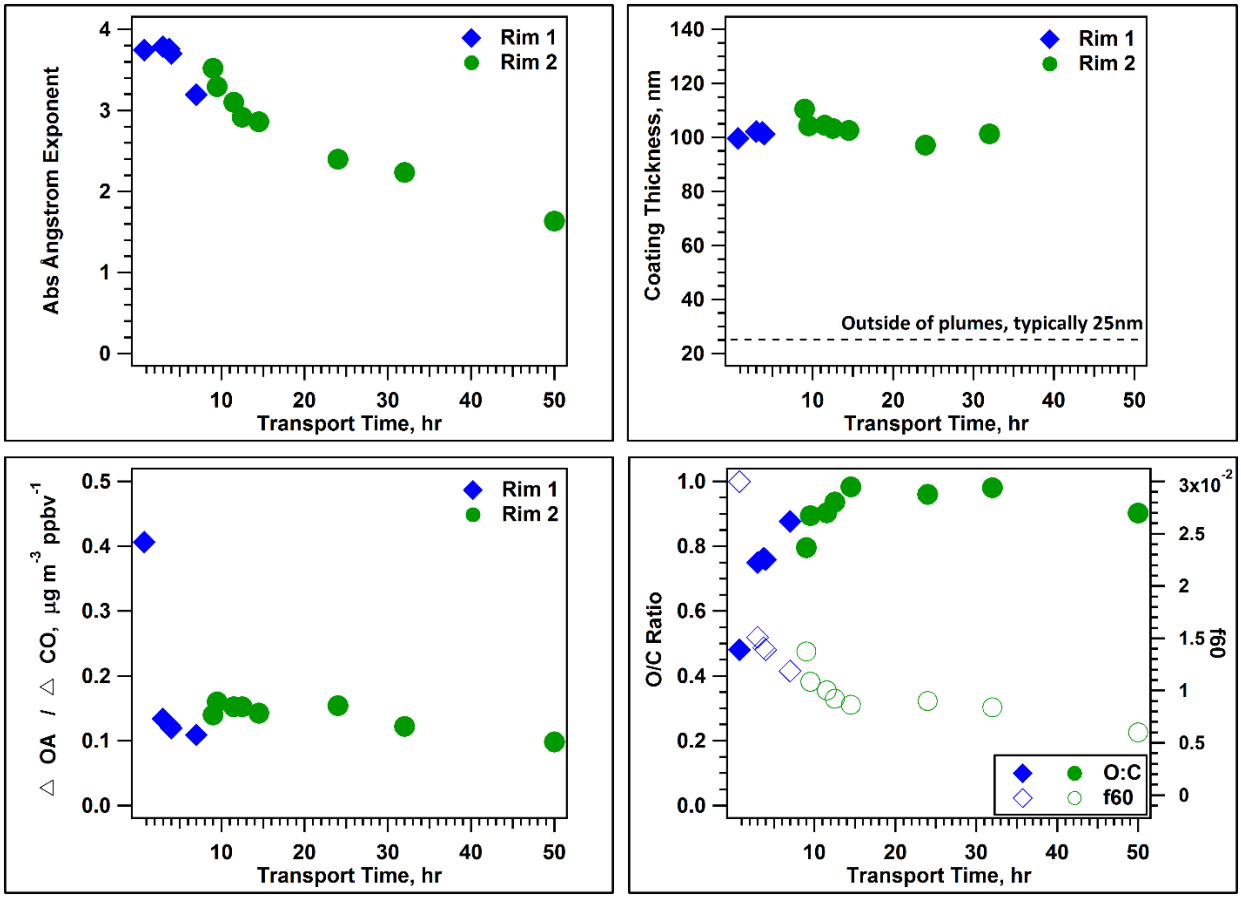

Figure 2.5: Evolution of other pertinent aerosol properties in Rim smoke plumes, including: (a) the AAE, (b) BC coating thickness, (c) ΔOA/ΔCO, and (d) OA oxygen-to-carbon ratio and f_{60} (tracer of biomass burning primary OA). Transport time for Rim 2 is calculated using the Elk Creek Complex fire source.

long ages, the approximate AAE for pure BC. The AAEs reach about 1.5 after 50 hours of transport, roughly the value recorded of background conditions in this study. This decrease in AAE highly correlates with the decrease in BrC, with $r^2 = 0.83$ (Figure 2.6a). The BC is highly coated in the plumes, with a coating thickness typically near 100 nm, significantly thicker than outside the plumes where it averages 25 nm. However, the coating thickness does not vary with plume age (Figure 2.5b), indicating the OA coating the BC particles must be non-volatile. Application of shell-and-core Mie theory has suggested that BC light absorption is enhanced with decreasing wavelength in a manner similar to BrC [*Bond et al.*, 2006; *Lack and Cappa*, 2010], so coatings might alter the light absorption spectral properties of BC. However, since both BC and the coatings atop BC were observed to be constant, the decrease in AAE with age must be due to the loss of some other light-absorbing compound—specifically, BrC—and cannot be explained by a shrinking shell over a BC core.

Since the chromophore-containing molecules that comprise BrC are expected to constitute a small mass fraction of bulk OA, differing trends in $\Delta OA/\Delta CO$ and $\Delta BrC/\Delta CO$ are not surprising (Figure 2.5c). OA initially decreases rapidly with a half-life of less than 2 hours, followed by little change after about 3 hours. In these plumes, evaporation losses apparently dominated over any secondary OA formation processes. Having a steady thickness of BC coating while bulk OA decreases is not inconsistent since the coating mass concentration is small relative to OA (estimated to be <10%, assuming OA and BC densities of 0.9 and 0.75 g cm^{-3}, respectively). In addition, OA is produced mainly by smoldering combustion, while BC is mainly by flaming combustion, thus the small fraction of OA associated with BC particles may have different composition from the bulk of OA coming from different processes in the fire. As the plume ages, the O/C (oxygenation) of the OA increases and f_{60} (biomass burning OA relative

to OA) decreases (Figure 2.5d), which has been previously observed [*Cubison et al.*, 2011]. The decay in f_{60} is likely due to a combination of evaporation and oxidation, as studied before [*Molina et al.*, 2004; *Robinson et al.*, 2007; *Lambe et al.*, 2012; *Donahue et al.*, 2014], and indicates that, although the bulk OA concentration stabilizes, its molecular composition changes with time. This is consistent with the evolving BrC. Indeed, the rate of change of both O/C and f_{60} better follow the decrease in BrC rather than the decrease of OA. The chemical transformations of the observed biomass burning OA, including changes in BrC, seem to occur approximately simultaneously, as indicated by correlations between the various variables (see Figure 2.6). Overall, this correlation between increasing O/C and decreasing BrC and f_{60}

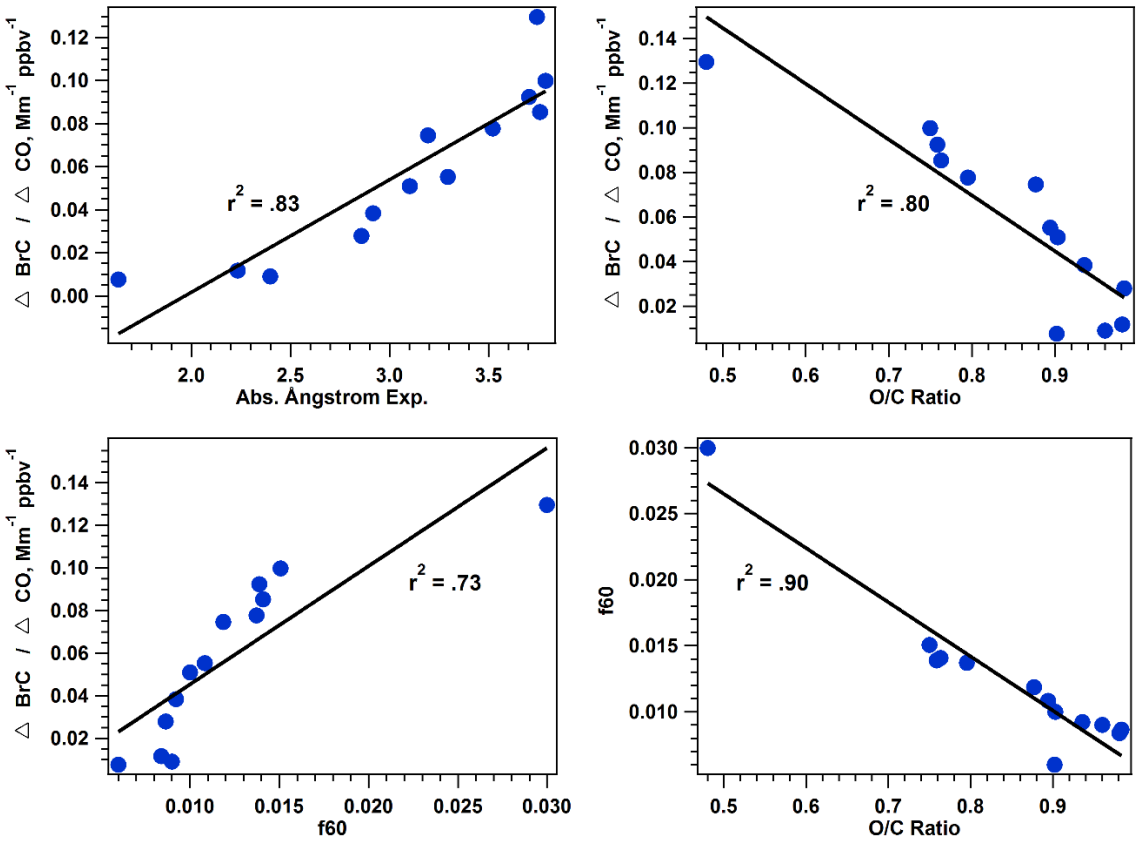

Figure 2.6: Correlations between: (a) ΔBrC/ΔCO and AAE, (b) ΔBrC/ΔCO and O/C, (c) ΔBrC/ΔCO and f60, and (d) f60 and O/C.

suggests a possible linked process, like photo-oxidation [*Zhao et al.*, 2015]. A photo-oxidation process leading to BrC loss is also consistent with the greater sunlight exposures correlating with decreases in BrC (Figure 2.4). Other processes could also be occurring, such as loss of volatile BrC. Further experiments and analyses of more ambient smoke plumes are needed to provide a better understanding of the life cycle of BrC from biomass burning.

2.4 Conclusions

The scale of the Rim 1 and 2 fires allowed for an unprecedented investigation into the evolution of wildfire smoke in the ambient atmosphere. These data show that absorption at 365 nm (Figure 2.4), and over the complete wavelength range associated with BrC, decreased with a half-life of roughly 9 to 15 hours. While the processes causing loss of BrC in the Rim smoke plumes combine to remove most emitted BrC within a day, this decay rate is typically far slower than losses observed solely due to photo-bleaching in current environmental chamber experiments with realistic conditions. However, both ambient and chamber data [*Lee et al.*, 2014; *Zhao et al.*, 2015; *Zhong and Jang*, 2014] imply that predictions of the prevalence or optical impacts of BrC cannot simply be inferred from emission or near-emission measurements without considering complex processing with age. Our data is unique in that plume evolution was observed over a sufficient time that a stable fraction of BrC was observed to persist. Approximately 6% of the emitted BrC remained above background levels even after 50 hours following emission and was no longer affected by sunlight. This BrC should be further investigated as it likely accounts for the ubiquitous BrC previously observed throughout the troposphere in a prior study with this aircraft payload, which was shown to have important radiative impacts [*Liu et al.*, 2014, 2015]. Since the total and relative impact of biomass burning on air quality is expected to increase [*Fuzzi et al*., 2015], future studies should focus on the

mechanisms responsible for the reduction of light absorption following biomass burning we observed and the difference in timescales with current laboratory experiments. Knowledge of the mechanisms governing behavior of BrC from biomass burning in the atmosphere would allow us to determine the overall climate forcing due to biomass burning BrC, and the degree to which it will affect air quality in general in the future.

CHAPTER 3

RADIATIVE FORCING DISCREPENCIES BETWEEN PREDICTED AND MEASURED PRIMARY BROWN CARBON

3.1 Introduction

Absorbing aerosols, like BC and BrC, can directly absorb incoming solar radiation and warm the planet. In contrast, scattering aerosols, including a majority of OA, directly scatter incoming solar radiation and cool the planet. Open biomass burning accounts for a large percentage of global primary OA (66%) and BC (33%) [*Bond et al*., 2004], with potentially significant impacts on climate warming. Biomass burning emissions travel through the troposphere, subject to meteorological conditions that affect transport, e.g., turbulence, and removal processes like wet and dry deposition, which alter the amount and properties of these emissions. These effects can mostly be accounted for in models. However, aerosol chemical and microphysical transformations also alter primary aerosols downwind of emission. These effects are more complicated to monitor, necessitating parameterizations in models that help track the beginning and end states of an aerosol's chemical, optical, and thermodynamic properties. The lifetime of BrC in the atmosphere has not been well characterized, mainly due to lack of data. Chapter 2 discussed how BrC absorption measured at 365 nm photobleaches after emission from wildfires. Any further optical changes in BrC with aging and transport are unknown. Therefore, the changes to the radiative forcing effects of BrC as it ages are also unknown. It is important to determine how the optical aging and transport of BrC affects its radiative forcing and how well its radiative forcing can be predicted using solely primary emissions.

In order to predict absorbing aerosol radiative effects, a constrained estimate of the complex refractive index (m = n – ik) of BC and OA needs to be determined. In the complex refractive index, the real part (n) indicates the scattering portion, and the imaginary part (k) describes the absorbing portion, or absorptivity. The complex refractive index can then be used to calculate the MAC and mass scattering cross-section, using a particle size distribution and Mie theory, which in turn can be applied to modeled concentrations of BC and OA to model their radiative forcing effects. The complex refractive index of BC has been relatively well characterized, especially in comparison to BrC, and was proposed by *Bond and Bergstrom* [2006] to be 1.95 – 0.79*i* at 550nm. Contrarily, the complex refractive index of OA was, until relatively recently, assumed not to have an imaginary part ($k_{OA} = 0$) due to the assumption that OA was solely a scattering aerosol. However, the absorbing portion of OA (BrC) has recently been found to span several orders of magnitude ($k_{OA} = 3x10^{-3} – 2x10^{-1}$) for fresh laboratory biomass combustion emissions [*Saleh et al.,* 2014], in agreement with other laboratory combustion measurements and atmospheric studies [*Lu et al*., 2015].

Furthermore, k_{OA} has been shown to correlate with the ratio of BC/OA, and the wavelength dependence of BrC also correlates with BC/OA [*Saleh et al*., 2014; *Lu et al.,* 2015]. This suggests that primary emissions of BC and OA from biomass combustion (such as wildfires) can be used to predict primary BrC emitted from biomass burning. Two studies have modeled the global radiative forcing of BrC using parameterizations that estimate BrC based on the BC/OA ratio [*Saleh et al*., 2014; *Lu et al.*, 2015]. Neither study has considered possible aging or transport effects downwind of a fire that might skew the radiative forcing results, such as photobleaching or photochemical transformations. In this chapter, the optical aging of BrC from fresh emissions to aged concentrations to background concentrations will be outlined next

to their radiative forcing effects to determine the degree to which aging and transport affect BrC radiative forcing and how well fresh primary emissions can parameterize aged concentrations. This will be done using BC and OA mass concentrations measured aboard an aircraft over the continental United States over the course of two summers as well as measured BrC spectrophotometric data collected simultaneously aboard the aircraft. The primary parameterization that the measured BrC will be compared to uses k_{OA} determined by a closure analysis of bulk light-absorption data [*Saleh et al.,* 2014], while the measured BrC filter method it is compared to uses light-absorption of liquid extracts from aerosol collected on filters [*Liu et al.,* 2014, 2015]. Therefore, some degree of disagreement is expected. However, the overall behavior should be consistent as long as the parameterization holds, so any deviations from expected behavior will be explained via references to BrC aging mechanisms, possible semi-volatility, and atmospheric transport.

3.2 Methods

The DC3 aircraft field campaign (May to June 2012) and the SEAC4RS aircraft field campaign (August to September 2013) collected a variety of atmospheric composition data products over western, central, and southeastern United States [*Toon et al.,* 2016]. A NASA DC-8 research aircraft with identical payload was used for both campaigns. Some differences between the flights exist: DC3 primarily set out to measure and study the convective transport of emissions and any chemical and compositional effects on the upper atmosphere post-convection, while SEAC4RS focused more on biomass burning, tropospheric chemistry, and Earth's radiative budget [*Toon et al.,* 2016]. Although both flights measured open biomass burning, SEAC4RS held specific flight objectives to measure biomass burning plumes over long timescales and a variety of source locations. A suite of gas and particle-phase instruments were

aboard the aircraft. However, due to the varied sampling times of the instruments, a time-merged data product was created on the NASA DC3 and SEAC4RS archives that merges all data products to the filter sampling time as long as the data covers more than 75% of the filter integration time.

3.2.1 Data Collection

Teflon filters collected aerosol with aerodynamic diameter less than nominally 4 μm [*McNaughton et al.,* 2007] for 5-10 minutes, before being stored at -10°C. Water extracts of the filters were made via 30 min of sonication in high-purity water. These extracts were then filtered and insoluble components removed with a 25 mm diameter .45 μm pore syringe filter (Fisher Scientific, Fisherbrand* Syringe Filters), to select for water-soluble BrC. Absorption measurements were obtained using a 2.5-m long Liquid Waveguide Capillary Cell (World Precision Instruments), a spectrophotometer with an ultraviolet-visible light source (200 to 900 nm wavelength range), and a light-absorption detector (Ocean Optics). The filter was drained and dried before re-extracting in methanol with 30 min of sonication, which selected for water-insoluble BrC. The light absorption of the water-insoluble portion was then measured via the same method as before. This method provides highly spectrally resolved absorption data for water-soluble and water-insoluble BrC, with the assumption that a combination of water and methanol dissolutions suffice to extract nearly all the BrC [*Chen and Bond,* 2010]. In Chapter 3, "BrC" measurements refers to total BrC, which is the water-soluble plus water-insoluble absorption averaged for 10 nm around the reported wavelength—e.g., BrC(365) denotes an average from 360-370nm. BrC absorption was calculated at a variety of wavelengths, from 200-700 nm with 33-nm step size.

OA and BC were measured simultaneously aboard the aircraft. OA mass concentrations

for aerodynamic diameter less than 1 μm were measured using a High Resolution Time of Flight AMS [*DeCarlo et al.,* 2006]. BC mass concentrations were made with an SP2 for the size range .09 micron to .55 micron, which accounts for 90% of the BC accumulation mode mass. The BC mass concentrations were corrected, using the methods from *Schwarz et al.* [2008], for particle sizes outside the measurement range. The SP2 directly measures refractory BC mass concentrations; this is reported as "BC" instead of "rBC" for comparison to other studies, which use the term "BC" to apply to SP2 data. CO mixing ratios were measured at 1-second time resolution using a differential absorption mid-infrared diode laser spectrometer containing a diode laser measuring the 4.7 μm CO absorption line [*Sachse et al*., 1987]. Acetonitrile (CH_3CN) mixing ratios were measured at a 15.75-second resolution using a Proton Transfer Reaction Mass Spectrometer.

3.2.2 Biomass Burning Period Selection

In order to delineate biomass burning events from background aerosol, we used CO and CH_3CN time series to determine periods of CO and CH_3CN enhancement above background values [*de Gouw et al.,* 2004]. When both measurements showed enhancement, the data was classified as biomass burning [see *Liu et al.,* 2014]. All non-burning data is referred to as background aerosol. Roughly 15% of the DC3 data (which contained 541 merged data points) and 13% of the SEAC4RS data (which contained 872 merged data points) were impacted by wildfire smoke, agricultural smoke, or significantly enhanced fossil fuel emissions during the campaign. Four SEAC4RS flights in particular measured both fresh and slightly aged wildfire smoke emissions whose initial fires and transport times could be calculated. The biomass burning-influenced and background air mass measurements are reported separately. For the following data descriptions, both campaigns used consistent methods of analysis.

For the biomass burning aerosol evolution data, transport times were calculated as in Chapter 2 solely for the time period corresponding to the highest smoke concentration for each plume pass during a flight, where the highest smoke concentration periods were determined using the CO time series. Subsequent back trajectories were performed using HYSPLIT to determine the fire source and time since emission for each intense smoke concentration above background. CO was used as a conservative tracer for normalized excess mixing ratios of extensive quantities, specifically BC mass (ΔBC/ΔCO). The days with determinable smoke transport times were: 6 Aug 2013 (from the Salmon River Complex fire, the Daves Fire, and the Dance/Orleans Fire, smoke spanning from southern Oregon down to California), 26 Aug 2013 (from the Rim fire at Yosemite, California, smoke spanning from California up into Idaho), 27 Aug 2013 (from the Elk Creek Complex fire, smoke spanning from Idaho up through Montana and into Canada), and 19 Sept 2013 (from separate fires at Yellowstone National Park in Wyoming, at Kansas, and at Oklahoma, smoke spanning all three states).

3.2.3 Optical Properties

In order to calculate the imaginary part of the refractive index (k_{OA}) from the BrC absorption data to compare against the BC/OA parameterization of k_{OA}, non-positive BC and OA values were removed. Using BrC absorption measurements, k_{OA}(550 nm) was calculated by:

$$kOA, 550 = \frac{550nm \times BrC(550nm) \times \rho}{4\pi\ OA} \quad (3.1)$$

For this study, a constant density of 1.5 g cm^{-3} was assumed; k_{OA} was calculated separately for both biomass burning events and background aerosol at a variety of wavelengths, from 200-700 nm, with 33-nm step size. A multiplicative factor of 2 is included to account for differences in direct absorption measurements of BrC versus Mie-predicted absorption assuming BrC remains in the accumulation mode, which is based on BrC size-distribution measurement comparisons

performed by *Liu et al.* [2013]; this factor has been used in other studies [*Liu et al.,* 2014, 2015]. Previous studies have also used a factor of .69-.75 and assumed BrC to be within the small particle limit [*Nakayama et al.,* 2013; *Sun et al.,* 2007]. For this study, this slight change in k_{OA} does not significantly affect our findings. The wavelength dependence of k_{OA} ($w = AAE_{BrC} - 1$) was calculated using the slope of a log-log plot of BrC absorption versus wavelength for the nominal wavelength region 350 to 500 nm; however, to avoid errors, this value was only used to study BrC optical aging mechanisms and not to calculate absorption at other wavelengths.

In order to compare the aging and optical behavior of our BrC measurements with predicted values using a ratio of BC/OA, the equations reported in *Saleh et al.* [2014] are used to calculate w and k_{OA}. Effectively, these equations calculate k_{OA} from the logarithm of the ratio of BC/OA and the wavelength dependence ($w = AAE_{BrC} - 1$) from the inverse of BC/OA. The *Saleh et al.* [2014] paper provides parameterizations for two assumptions: an external mixing case, where BC and BrC absorption are separate; and an internal mixing case, where BrC absorption occurs as a coating atop BC particles. Both parameterizations are considered and compared against in this paper, although the external mixing case is more directly comparable to the BrC absorption filter measurements.

Total aerosol light-absorption coefficients ($b_{ap}(\lambda)$) and light-scattering coefficients ($b_{sp}(\lambda)$) were measured by a Radiance Research Particle Soot Absorption Photometer (PSAP) and a TSI-3563 nephelometer, respectively. Artifacts caused by filter-based optical absorption measurements were corrected for by the method described in *Virkkula et al.* [2010]. The wavelength dependence of the absorption was calculated using absorption coefficients at 470 nm and 532 nm, due to lack of 660 nm absorption measurements during the SEAC4RS campaign. The bulk aerosol AAE, which considers the combined absorption by BrC and BC at two separate

wavelengths, can be calculated as in Eq. 2.1. AAE were only calculated for times when $b_{ap}(470)$ and $b_{ap}(532)$ both exceeded 1 Mm^{-1}. Once the contribution by BrC absorption was subtracted out, the bulk aerosol absorption at 532 nm was used to calculate BC absorption at a variety of wavelengths from 200-700 nm with 33-nm step-size, using an AAE of 1 and the inverse of Eq. 2.1. The scattering Ångström exponent (SAE) provided in the merged data set of optical constants was used to compute scattering coefficients at a variety of wavelengths from 200-700 nm with 33-nm step-size, using the scattering coefficient reported at 550 nm, b_{sp}(550 nm):

$$b_{sp}(\lambda) = b_{sp}(550)\left(\frac{550\,nm}{\lambda}\right)^{SAE} \quad (3.2)$$

The scattering coefficient, BrC absorption coefficient, and BC absorption coefficient were used to calculate aerosol optical depth and single-scattering albedo for input into the Santa Barbara DISORT Atmospheric Radiative Transfer (SBDART) model to determine the downwelling flux, upwelling flux, and radiative forcing associated with BrC [*Ricchiazzi et al.,* 1998].

3.3 Biomass Burning and Background Aerosol Measurements

If the predicted and measured BrC absorption is to be comparable more than an hour downwind of a smoke plume, then their evolutionary cycle needs to be consistent. In Figure 3.1, the absorptivity of OA is plotted versus time, showing that k_{OA}(550 nm) decreases exponentially over time from near-emission to stability, with an e-folding time τ of 8.7 hrs (with a range of 7-12 hrs). This rate of decrease remains independent of the fire source: plumes followed along their path of aging in a quasi-Lagrangian experiment (Aug. 26 and Aug. 27 data) decrease at the same rate as plumes from separate fires (Aug. 6 and Aug. 19 data), for smoke measured in the continental United States. This decrease in k_{OA} is a direct result of decreasing BrC absorption due to photobleaching (Chapter 2). However, secondary effects like evaporation (or volatilization) could also factor into this decrease in k_{OA}. Variations from the exponential decay

curve are typically correlated with altitude: higher altitude biomass burning data are underestimated by the exponential fit while lower altitude data are overestimated. Typically, radiative forcing models treat k_{OA} as a constant value with possible lower and higher values caused by combustion conditions [*Chen and Bond*, 2010; *Saleh et al*., 2015; *Feng et al*., 2013]. However, the fact that k_{OA} decreases over time (Figure 3.1) brings into question the treatment of k_{OA} as a set value several hours after emission in models of biomass burning radiative forcing.

Recently, k_{OA} measurements and *w* have been predicted using emission characteristics of BC/OA in models of radiative forcing for biomass burning aerosols [*Saleh et al.,* 2015; *Lu et al*.,

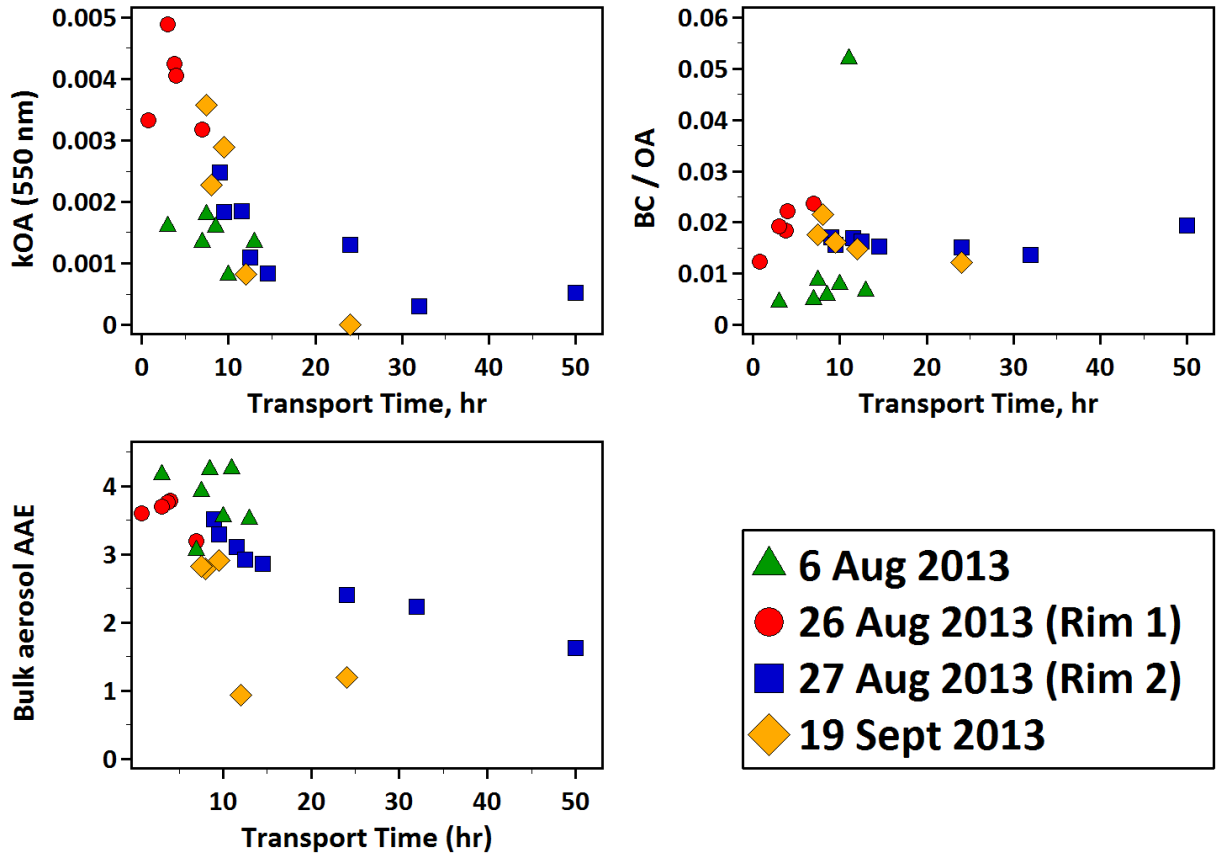

Figure 3.1: The comparative evolution of measured OA absorptivity (k_{OA}), the fire emission characteristics substitute that will be used to predict k_{OA} (BC/OA), and bulk aerosol AAE during SEAC4RS smoke plumes.

2015]. Near fires, the mass ratio BC/OA reflects the relative fine mode contributions of the BC and OA emissions and thus the burn conditions of the fire, whereas higher BC emissions (and thus BC/OA ratios) occur during flaming fires [*Reid and Hobbs,* 1998] and higher OA emissions (lower BC/OA ratios) during smoldering fires [*Yokelson et al.,* 1997]. To be comparable with the measured k_{OA}, these predictions of k_{OA} using BC/OA need to show similar evolution over time. Nevertheless, Figure 3.1 shows that the ratio of BC/OA remains static as the plume ages despite changing k_{OA} values. The measurements for multiple-fire smoke plumes show some variation in the BC/OA ratio, but this is solely due to the large amounts of OA encountered during the Aug. 6 smoke measurements, likely caused by secondary OA formation outweighing OA evaporation. Ignoring this atypical behavior, the BC/OA remains relatively constant over plume age, suggesting that a source profile of smoke emissions or a measure of a fire's burn conditions in the continental United States may not be accurate in predicting k_{OA}, and thus OA absorption, downwind of plumes. Specifically, any parameterization depending k_{OA} on the behavior of BC/OA should fail after roughly 3 hrs of aging.

For external evidence of this OA absorptivity decrease, the bulk aerosol AAE is plotted as a function of transport time in Figure 3.1. Bulk aerosol AAE is indicative of the relative difference between the ultraviolet and visible wavelengths and is shown to decrease over time for all fire sources. This could result from a decrease in BrC absorption, a decrease in BC absorption, or a decrease in the organic coatings atop BC. In Chapter 2, it was shown that both BC mass and the coating thickness atop BC remain relatively constant over plume age for single-fire measurements (Aug. 26 and Aug. 27 data), so the absorption by BC should be constant for these data. Therefore, the only reason behind the decrease in bulk aerosol AAE for single-fire

measurements is that k_{OA} —whose behavior is controlled by BrC absorption—is decreasing. Despite this link between the two optical properties, the bulk aerosol AAE decreases at a much slower rate than k_{OA}. This is caused by a non-constant spectral change of the BrC. If plotted for each period of time in the single-fire plume, the normalized absorption spectrum for BrC shows a

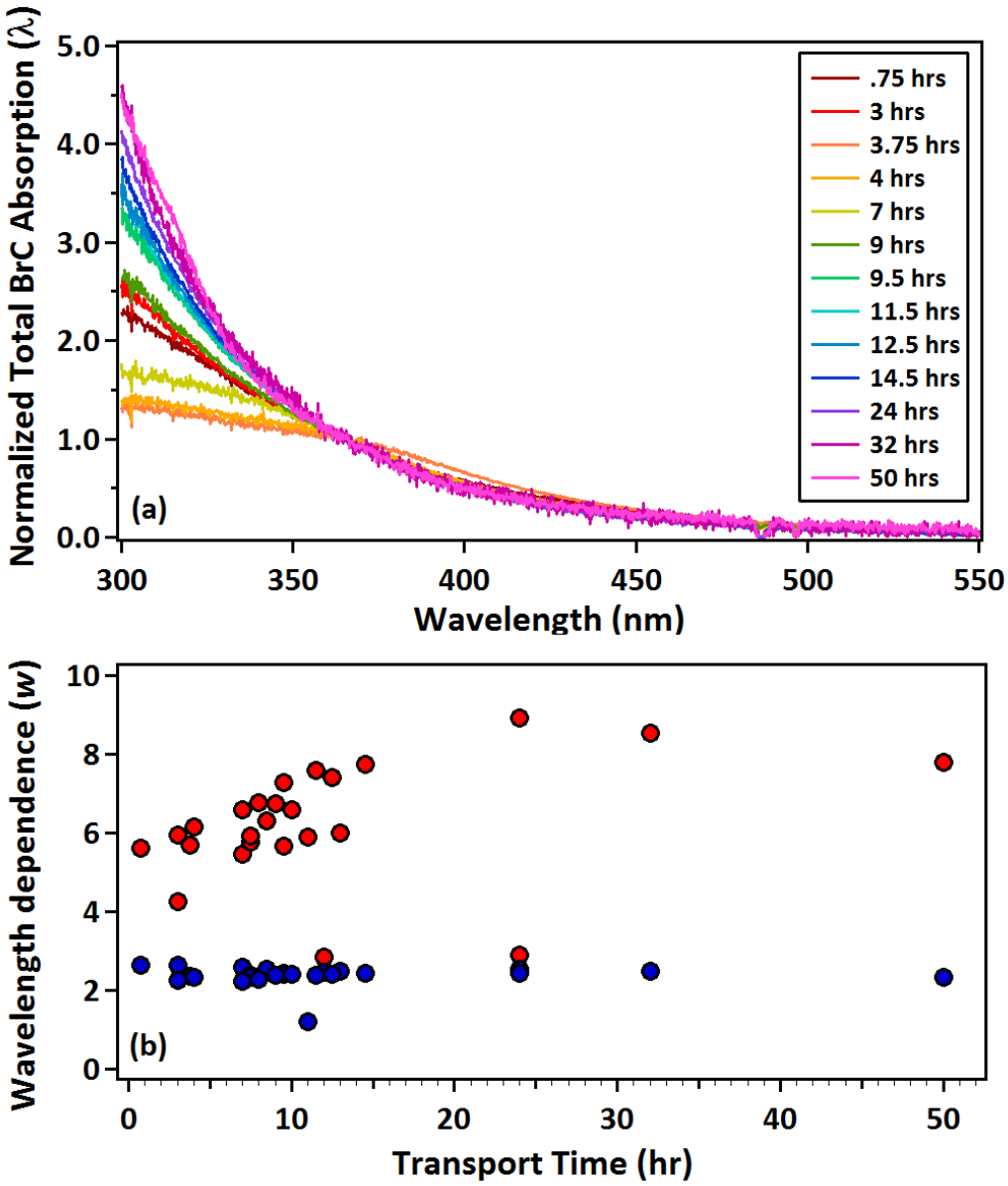

Figure 3.2: The evolution of (a) BrC absorption spectra, and (b) the wavelength dependence of k_{OA}.

steeper curve from 300-350 nm for aged smoke than fresh smoke (Figure 3.2a). Quantitatively, the wavelength dependence of k_{OA} ($w = AAE_{BrC} - 1$) actually increases as it ages, from roughly 6 to 9 (Figure 3.2b). Although this difference may seem small, it has important effects:

1. This "aging" of the k_{OA} wavelength dependence (and BrC AAE) likely accounts for the dissimilar rates of decrease for k_{OA} and bulk aerosol AAE.
2. The AAE of BrC is typically considered to be a single value for a given set of combustion conditions, which is then used to calculate BrC absorption at non-measured wavelengths. If the AAE of BrC is increasing while BrC absorption is decreasing, modeling the absorption of BrC and its radiative effects post-emission from biomass burning becomes significantly more difficult.

This increase in BrC AAE is likely due to aging of the chromophores, e.g. photochemical reactions causing decreases in molecules that absorb light at ultraviolet wavelengths in a disproportionately larger amount than those molecules that absorb light in the visible wavelengths. Furthermore, previous studies have shown that fresh biomass burning emissions had a linear correlation between *w* and the ratio of BC/OA [*Saleh et al*., 2014; *Lu et al.,* 2015]. Figure 3.2b shows that attempting to predict *w* from a correlation with BC/OA grossly underestimates the measured, changing values of *w*. Therefore, future modelers should be careful when using static wavelength dependence parameterizations if any aging beyond 3-4 hrs has affected the biomass burning emissions.

To assess agreement between measured and predicted BrC, using the *Saleh et al*. [2014] parameterization as an example, k_{OA} is plotted against BC/OA in Figure 3.3 using airborne biomass burning measurements from DC3 and SEAC4RS. The parameterization of k_{OA} as a

function of BC/OA is plotted for the range of BC/OA values from DC3 and SEAC4RS (.001 to .1). The fresher biomass burning predicted k_{OA} behavior correlates decently well with measured k_{OA}, despite being a consistent half to two orders of magnitude larger. As the smoke ages past 10 hrs, the measured k_{OA} begins to deviate from the expected trend of the

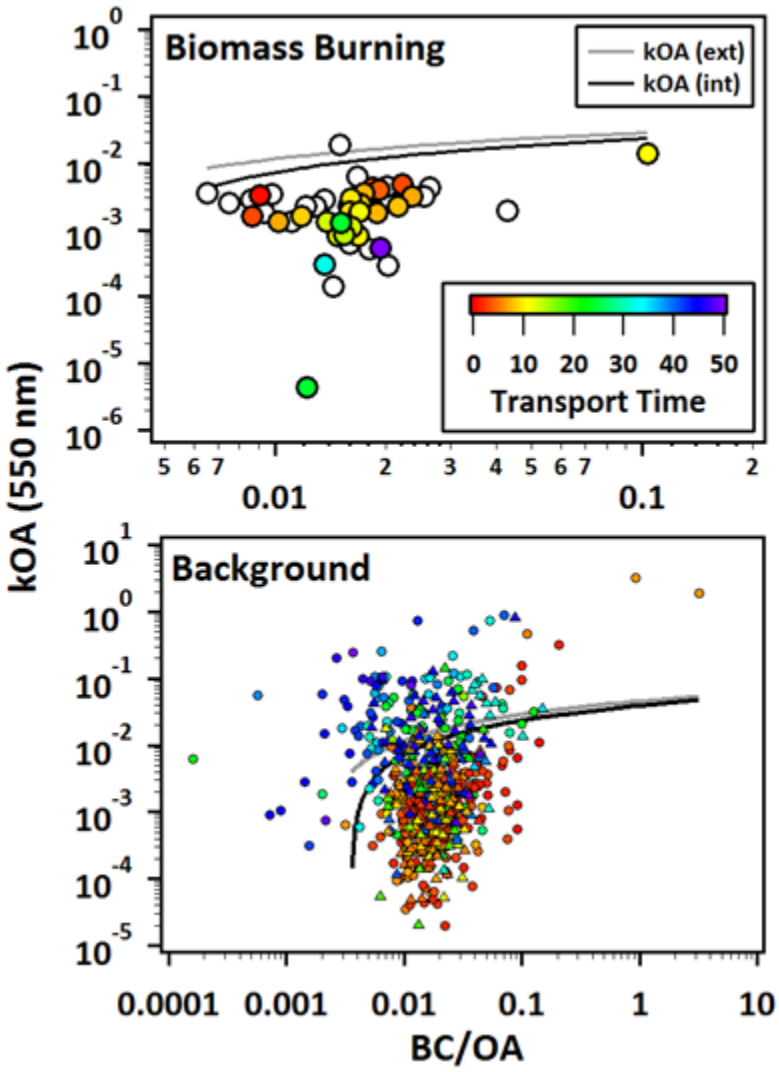

Figure 3.3: Values of k_{OA} for both biomass burning and background atmospheric measurements; grey line indicates the *Saleh et al.* (2014) external mixing assumption and black the internal mixing assumption.

parameterization, incurring disagreements of 2-3 orders of magnitude. Differences across several orders of magnitude can have significant effects on radiative forcing calculations, so this disagreement is concerning. The exponential decay of BrC as it ages is likely causes the deviation, suggesting well-aged regional aerosol may largely deviate from the parameterization.

Well-aged background BrC aerosol is a mixture of combustion from fossil fuels and biomass burning as well as possible secondary BrC. Since the parameterizations of k_{OA} as a function of BC/OA are specifically only for biomass combustion and not fossil fuels [*Saleh et al.,* 2014], the k_{OA} of background aerosol would not be expected to have the same linear correlation between k_{OA} and BC/OA as biomass combustion. Nevertheless, plotting background aerosol k_{OA} versus BC/OA is necessary in order to understand how aging may affect the comparability between predicted and measured k_{OA}. Figure 3.3 shows that measured background aerosol k_{OA} from the continental United States spans several orders of magnitude—as expected considering the range of k_{OA} for different combustion sources—but does not correlate with BC/OA. Yet, if we consider the altitude at which the BrC was measured, a pattern appears. Higher-altitude measured k_{OA} is underestimated by the predicted k_{OA} while lower-altitude measured k_{OA} is overestimated by the predicted k_{OA}. This altitude profile is significant: higher altitude k_{OA} in the continental United States is several orders of magnitude higher than fresh biomass burning k_{OA} (Figure 3.3). If future modelers aim to predict k_{OA} or BrC based solely on reported BC/OA for background aerosol in the continental United States, some temperature or altitude dependence likely needs to be considered.

To investigate these altitude effects, Figure 3.4 shows the altitude profiles for background aerosol k_{OA} and BC/OA. An obvious increase in k_{OA} with altitude by roughly one order of magnitude is not shared by the aerosol ratio of BC/OA, which remains relatively constant. This

enhancement of OA absorptivity with altitude is consistent with previous observations over the continental United States using the DC3 data where the ratio of BrC to BC absorption was found to increase with altitude [*Liu et al.,* 2014], since BrC/BC is mathematically equivalent for filter extract absorption measurements with k_{OA}/(BC/OA). It should be noted that there is no a priori reason to expect BC and OA to remain highly correlated with altitude, nor is there reason to expect OA absorptivity (or BrC absorption) enhancement with altitude. This enhancement is significant: high-altitude background aerosol k_{OA} has larger values than fresh or aged smoke, while low-altitude background aerosol has equal or lower values than fresh or aged smoke. Typically, we would expect fresh biomass to have the largest OA absorption, especially if photobleaching affects all emitted BrC. However, if the absorption of the aerosol is considered relative to its mass, OA absorptivity becomes largest at high altitudes where there is less OA but more BrC by mass. Some evidence exists suggesting BrC can be formed secondarily in clouds [*Nguyen et al.,* 2012, *Desyaterik et al.,* 2013] and is, in fact, enhanced by convection with relation to BC and OA [*Zhang et al.,* 2017]. Therefore, the vertical profiles in Figure 3.4 could result from differing mechanisms of cloud processing between BC, OA, and BrC, e.g., cloud processing predominantly removing BC and OA in the upper atmosphere via precipitation while forming BrC through aqueous secondary OA reactions. *Zhang et al.* [2017] also proposes that BrC aerosol may have slightly higher size distributions than BC and OA, resulting in precipitation removing more BC and OA than BrC; this could cause the vertical profile of BrC to be enhanced with altitude in comparison to BC and OA. Evidence for this is derived from *Liu et al.* (2013) comparing BrC size distributions to BC size distributions, where there is noticeable BrC above the typical 2.5 micron cutoff diameter. Contrarily, the vertical profile may be largely dependent on the volatility of the aerosol. If some BrC molecules are semi-volatile, then the

colder temperatures at higher altitudes could result in condensation of BrC and, thus, higher k_{OA} at high altitudes. The biomass burning evolution graph of k_{OA} (Figure 2.4) suggests this may be a possibility, since higher-altitude k_{OA} has higher values than expected for the given smoke age. However, freshly combusted BrC measured in a smog chamber has previously been found to have extremely low volatility [*Saleh et al.,* 2014], as has brown aqueous secondary OA [*Laskin et al.*, 2015]. Therefore, the only volatile BrC is likely the aged biomass combustion BrC or BrC formed from fossil fuels. It should be noted that these mechanisms may be affected by transport phenomena unique to the continental United States. Further study of brown carbon vertical

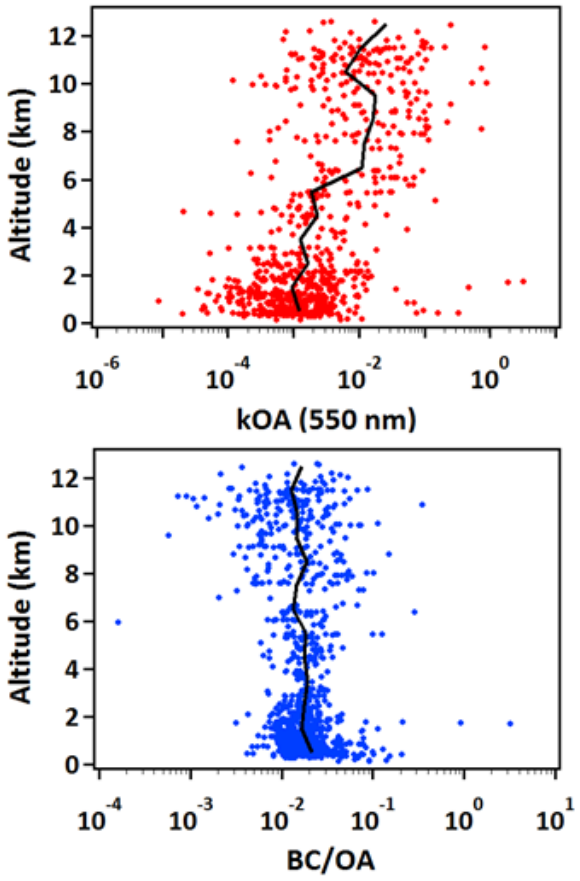

Figure 3.4: Background aerosol altitude profiles, with median (black line), for DC3 and SEAC4RS.

profiles in other regions with differing transport phenomena needs to be made.

3.4 Radiative Forcing

In the previous section, predicted k_{OA} from fresh biomass burning correlated relatively well with measured k_{OA} while aged smoke and background aerosol correlated poorly. In order to determine how significant these differences between predicted and measured BrC are to the climate effects and radiative forcing of BrC, both fresh smoke, aged smoke, and background BrC aerosol need to be expressed in terms of radiative forcing and then compared. To determine BrC radiative forcing, SBDART was used to model the radiative imbalance (downwelling flux – upwelling flux) for a vertical profile of aerosol, created for various conditions, in a mid-latitude summer at a 40° solar zenith angle, following *Liu et al.* [2014]. Vertically-resolved aerosol optical properties (BC absorption, BrC absorption, and scattering coefficient) were determined for 33-nm intervals between 300-700 nm using: BC absorption predicted at a variety of wavelengths using bulk aerosol absorption at 532 nm and an AAE of 1; measured BrC absorption spectra; and scattering coefficients calculated for a variety of wavelengths using the SAE. The mean of the BrC absorption spectra at each altitude was used, rather than the median as shown in Fig. 4, to be consistent with previous studies [*Liu et al.,* 2014, 2015].

Total absorption and scattering coefficients were determined for each of three cases, following the method of *Liu et al.* [2015]: 1) only scattering aerosols, 2) scattering aerosols and BC, and 3) scattering aerosols, BC, and BrC. Aerosol optical depth and single-scattering albedo calculated from the absorption and scattering coefficients, in addition to a wavelength-independent asymmetry parameter of 0.65 [*Carrico et al.*, 2003], were used as inputs to SBDART. Radiative forcing (RF) was calculated as the difference between the radiative imbalance of some absorbing aerosol species (e.g., BC) and the radiative imbalance of all the

scattering species. The following cases were considered for both the measured BrC and the predicted BrC (using the *Saleh et al.* [2014] parameterization):

1. **Background aerosol:** the measured background aerosol was used to calculate the base vertical profile for SBDART, using the data mean for each 1-km altitude bin.
2. **Fresh biomass burning plumes:** the fresh biomass burning plumes (age < 3 hrs) measured during SEAC4RS spanned 0 to 4 km of well-mixed aerosol, as determined by lidar data of the region below the airplane. This smoke aerosol was assumed to have constant aerosol optical properties throughout this plume thickness. Altitudes from 5 to 12 km were considered the same as the background case.
3. **Aged biomass burning plumes:** the aged biomass burning plumes (age > 14 hrs) measured during SEAC4RS spanned 2.5 to 4.5 km of well-mixed aerosol, as determinable from lidar data of the region above and below the airplane. Once again, smoke aerosol was assumed constant throughout plume thickness. Altitudes 0.5 to 2.5 km and 4.5 to 12 km were considered the same as the background case.

By considering these scenarios separately, the relative importance of aging mechanisms (such as photobleaching) versus transport mechanisms (that cause the altitude dependence) to modeling radiative forcing of BrC become obvious. Further, by calculating each scenario for predicted BrC as well as measured BrC, the degree to which a parameterization of k_{OA} based on BC/OA will succeed in determining BrC radiative forcing can be ascertained. The wavelength dependence of k_{OA} was calculated using the parameterization set forth in *Saleh et al.* [2014], which was shown in Figure 3.2b to disagree with the measured spectral *w*. This *w* is then used to calculate k_{OA} at non-550-nm wavelengths, causing an insignificant amount of disagreement.

Exact values of radiative forcing are reported for the top of the atmosphere (TOA, determined at 15 km) in Table 3.1. For background aerosol, BrC is shown to account for a significant portion (26%) of the total forcing by absorbing aerosols (BrC + BC), which is consistent with previous calculations for this data [*Liu et al.*, 2015; *Zhang et al.*, 2017]. However, BrC RF is overestimated by the predicted BrC values by 1.6 W/m^2. Thus, while BrC actually contributes roughly 25% to absorbing aerosol RF at TOA for background aerosol, the parameterization finds only 45.6% due to absorbing aerosol RF (Table 3.1). This is largely driven by the prediction not capturing the BrC absorption enhancement with altitude. This disagreement suggests that, for background aerosol, BrC absorption should not be parameterized by BC/OA; modelers should be careful to use BC and OA data only from biomass burning emissions.

From Figure 3.1 and Figure 3.3, fresh biomass burning smoke is expected to have good agreement between measured and predicted BrC radiative forcing, while aged smoke should have poor disagreement. Indeed, when quantified as the percent BrC contributes to absorbing aerosol RF, the model shows that measured fresh biomass burning BrC accounts for 6% of the RF at TOA while the predicted BrC estimates 12% is due to BrC (Table 3.1). This factor of 2 difference is likely due to the nearly 2 orders of magnitude difference in the predicted and measured k_{OA} values. Inside the smoke plume itself, measured fresh biomass burning BrC only contributes roughly 5% to the total absorbing aerosol RF while the predicted BrC estimates it accounts for 7% of the forcing (Table 3.1). Overall, the radiative forcing of fresh smoke emissions are relatively well predicted using the *Saleh et al.* [2014] parameterization. However, calculating TOA radiative forcing using the parameterization will likely result in some errors due

Table 3.1: Radiative forcing at top of the atmosphere

Radiative Forcing at TOA (W/m^2)		Fresh Smoke	Aged Smoke	Background
BC	Measurements	270.12	4.84	3.37
	Parameterization	270.12	4.84	3.37
BrC	Measurements	17.32	1.62	1.21
	Parameterization	35.44	4.13	2.82
BrC/BrC+BC	Measurements	6.0%	25.0%	26.4%
	Parameterization	11.6%	46.0%	45.6%

to an inappropriate grasp of the background aerosol with altitude, since high-altitude background BrC is shown to significantly affect RF [*Zhang et al.*, 2017]. The difference between the parameterization and measurements is more pronounced for aged smoke. Measured BrC accounts for 25% of the absorbing aerosol RF at TOA, while the predicted BrC estimates 46% (Table 3.1). Most of this difference is due to the BrC vertical profile, which affects the atmosphere in the profile outside of the smoke plume inserted from 3-4 km. Inside the plume itself, measured BrC accounts for roughly 54% of the absorbing aerosol RF, while predicted BrC estimates that BrC contributes to 47% of the absorbing aerosol RF.

The difference between measured and predicted absorption inside the plume is much smaller for both fresh and aged smoke, suggesting the slight RF overestimation by predicted BrC absorption is probably acceptable for many applications. Photobleaching, while significant, is less important for a radiative forcing model to capture than the vertical profile of BrC, at least in the continental United States. Indeed, if the altitude profile of BrC is not properly captured by a model (as with the predicted BrC), the contribution of BrC to absorbing aerosol RF at TOA in

regions with similar atmospheric transport as the United States will likely be greatly overestimated by a little less than a factor of 2.

3.5 Conclusions

The decrease in k_{OA} (describing the absorptivity of OA, which is correlated with BrC absorption) of a smoke plume as it ages is complicated by the increasing of the wavelength dependence of k_{OA} with age. This, in turn, affects the predictability of BrC absorption downwind of emissions from biomass burning due to overall absorption decreasing while absorption in the ultraviolet decreases slower than in the visible wavelengths. After roughly 14-24 hrs, both the k_{OA} and wavelength dependence have stabilized, allowing for the optical effects of aged smoke to be better predicted. Recent parameterizations of k_{OA} and its wavelength dependence based on BC/OA, can be used for fresh biomass burning emissions, less than a couple days old, to predict radiative forcing inside of a smoke plume. However, outside a smoke plume, these predictions fall apart because the altitude profile of BC/OA does not capture the enhancement of k_{OA} with altitude. These parameterizations cause a consistent overprediction of BrC radiative forcing by nearly a factor of 2 for data taken in the continental United States. The degree to which this affects TOA radiative forcing of smoke plumes depends on the amount of absorption inside the smoke plume, causing fresh smoke to have the largest BrC radiative forcing at TOA since it has the largest amount of BrC in the plume. Radiative forcing of BrC at TOA for aged smoke (1-2 days) was roughly that of the background aerosol, due to the absorption inside the low-altitude plume being relatively small in comparison to high-altitude background aerosol.

The most important factors for calculating the radiative forcing of BrC are: 1) the time since the aerosol was emitted, since the greatest radiative forcing for BrC is in the first couple of hours when BrC has not yet been photobleached and depleted, and 2) the altitude at which it was

measured, since higher altitudes showed significant enhancement of k_{OA} in the continental United States. In the future, models of BrC radiative forcing—which affects background aerosol radiative forcing as a whole, since BrC accounts for 26% of background absorbing aerosol radiative forcing—need to find a way to account for the altitude enhancement of BrC in order to correctly calculate its absorption. Models using vertically-resolved satellite measurements over the continental United States also need to account for this altitude dependence since it affects their retrieval algorithms for BC versus BrC absorption.

CHAPTER 4

CONCLUSIONS AND FUTURE WORK

4.1 Conclusions

The first part of this thesis (Chapter 2) presented the first results of BrC evolution after emission from a wildfire. BrC was shown to decrease over time while BC and OA, two aerosols with similar formation mechanisms, remained constant with plume age. An external measure of light absorption, the bulk aerosol AAE, was also shown to decrease with time, suggesting that the decrease in BrC absorption caused the bulk aerosol AAE to also decrease. While high r^2 correlations were shown between BrC, the bulk aerosol AAE, OA O/C ratio, and f_{60}, these comparisons only hold true for single-fire biomass burning measurements. For smoke plumes across a variety of different fire sources, O/C and f_{60} show no correlation with BrC, and the correlation between AAE and BrC is surprisingly non-linear. Some of these disagreements may be based on aerosol age (as with AAE and BrC) while others may be caused by atmospheric conditions and source fire material (O/C and f_{60}).

The second part of this thesis (Chapter 3) showed that the absorptivity of OA (k_{OA} which is essentially BrC/OA) also decreases with plume age but at a separate rate from the bulk aerosol AAE. The difference in decay rates is due to the changing nature of the wavelength dependence of k_{OA} ($w = AAE_{BrC} - 1$), where w increases over the course of 9 hrs by a difference of 2. This complicated nature of BrC absorption decreasing over time while the differential between the ultraviolet and visible wavelength absorption of BrC increases over time causes problems for static assumptions of BrC AAEs and predictions of BrC absorption at non-observed wavelengths. In addition, Chapter 3 shows that predictions of k_{OA} based on BC/OA ratios work

decently well for fresh biomass burning, but not for aged biomass burning or background aerosol. This is caused by a combination of aging, causing a decrease in k_{OA} over time while BC/OA and thus predicted k_{OA} stays constant, and transport, whereby higher-altitude k_{OA} are underestimated by predicted k_{OA} and lower-altitude k_{OA} are overestimated by predicted k_{OA}.

Future modelers of BrC, whether for radiative forcing modeling or BrC chemical transport models, should take into account the following insights from this thesis:

- BrC absorption and k_{OA} decrease over time post-emission from biomass burning
- The wavelength dependence (AAE) of BrC and k_{OA} increase after emission
- BrC aging behavior is not shared with other similar species (BC and OA)
- k_{OA} can be parameterized in the atmosphere by BC/OA for fresh and aged fires
- k_{OA} should not be parameterized for background aerosol outside a smoke plume

A model considering these qualities should capture actual BrC behavior well. For most applications, the increase in the AAE of BrC with age post-emission from a fire should be insignificant. However, any assumption of a static AAE for a large group of BrC from biomass burning is likely false. It should be noted that the measurements in Chapter 3 were made using data from the continental United States, so the transport phenomena underlying the vertical profiles of k_{OA} may be unique to continental regions or certain latitudes. Models done over areas with vastly different atmospheric transport mechanisms would need to address an assumption of consistency between the modeled areas and the location of this data set.

4.2 Future Work

As a first-look at BrC optical evolution, this work brings about many opportunities for further research. While both fresh and slightly aged biomass burning aerosol were studied (from 0.75 to 50 hrs old), well-aged biomass burning could not be identified. Any changing optical

properties and continued aging of BrC past this point is unknown, and it is possible that the BrC could continue being photobleached and disappear altogether or that secondary BrC is formed in well-aged plumes so that any photobleaching is counterbalanced by BrC formation in the diluting plume. In addition, the increase in the wavelength dependence of BrC absorption suggests that not all BrC molecules respond similarly to photobleaching. Further studies on the molecular weights and species of these molecules could yield valuable insights into both primary and secondary BrC. The volatility of any aged biomass burning BrC and secondary BrC is also largely unknown. Experiments that look into optical and molecular response of BrC to changes in temperature would likely yield valuable insights into the altitude profile of BrC. However, simultaneous measurements of corresponding theories—including size distribution changes—would also need to be made, all of which is complicated by any further aging and photochemical mechanisms that could alter the BrC aerosol. However, finding the root cause behind the enhancement of BrC absorption with altitude is paramount to predicting BrC absorption in background aerosol, so it is a significant area of future BrC research.

Furthermore, although investigations into the vertical profiles of BrC over the continental United States has been completed, expansive research into BrC profiles over the ocean and over regions far removed from biomass burning influence still need to be conducted. Such studies would help confirm whether the vertical profiles of BrC discussed in Chapter 3 are globally consistent or whether these phenomena are localized to continental land masses with well-mixed tropospheric aerosol that sources significant amounts of biomass burning. This aged biomass burning, once transported to different altitudes, likely accounts for the vertical profiles of BrC. Without local biomass burning sources on the continent, the vertical profile may be less prominent despite long range transport of biomass burning aerosols.

REFERENCES

Aiken, A.C., DeCarlo, P., Kroll, J.H., Worsnop, D.R., Huffman, J.A., Docherty, K.S., Ulbrich, I.M., Mohr, C., Kimmel, J.R.Sueper, D. 2008. O/C and OM/OC ratios of primary, secondary, and ambient organic aerosols with high-resolution time-of-flight aerosol mass spectrometry. *Environ. Sci. Technol.*, 42: 4478–85. doi:10.1021/es703009q

Andreae, M. O. and Gelencsér, A. (2006): Black carbon or brown carbon? The nature of light-absorbing carbonaceous aerosols, *Atmos. Chem. Phys*., 6, 3131–3148, doi:10.5194/acp-6-3131-2006.

Aquila, V., Hendricks, J., Lauer, A., Riemer, N., Vogel, H., Baumgardner, D., Minikin, A., Petzold, A., Schwarz, J. P., Spackman, J. R., Weinzierl, B., Righi, M., and Dall'Amico, M.: MADE-in: a new aerosol microphysics submodel for global simulation of insoluble particles and their mixing state, Geosci. Model Dev., 4, 325–355, doi:10.5194/gmd-4-325-2011, 2011.

Bergstrom, R. W., P. Pilewskie, J. Pommier, M. Rabbette, P. B. Russell, B. Schmid, J. Redemann, A. Higurashi, T. Nakajima, and P. K. Quinn (2004), Spectral absorption of solar radiation by aerosols during ACE-Asia, *J. Geophys. Res*., 109, D19S15, doi:10.1029/2003JD004467.

Bond, T. C. (2001), Spectral dependence of visible light absorption by carbonaceous particles emitted from coal combustion, *Geophys. Res. Lett.*, *28*, 4075– 4078. doi: 10.1029/2001GL013652

Bond, T. C., et al. (2004), A technology-based global inventory of black and organic carbon emissions from combustion, *J. Geophys. Res*. 109, D14203. DOI: 10.1029/2003/JDO03697.

Bond, Tami C. and Bergstrom, Robert W.(2006) 'Light Absorption by Carbonaceous Particles: An Investigative Review', *Aerosol Science and Technology*, 40: 1, 27 — 67, DOI: 10.1080/02786820500421521

Bond, T. C., G. Habib, and R. W. Bergstrom (2006), Limitations in the enhancement of visible light absorption due to mixing state, *J. Geophys. Res.*, *111*(D20211), doi:10.1029/2006JD007315.

Bond, T. C., et al. (2013), Bounding the role of black carbon in the climate system: A scientific assessment, *J. Geophys. Res. Atmos*., 118, 5380–5552, doi:10.1002/jgrd.50171.

Bones, D. L., D. K. Henricksen, S. A. Mang, M. Gonsior, A. P. Bateman, T. B. Nguyen, W. J. Cooper, and S. A. Nizkorodov (2010), Appearance of strong absorbers and fluorophores

in limonene-O3 secondary organic aerosol due to NH4+-mediated chemical aging over long time scales, *J. Geophys. Res.*, 115, D05203, doi:10.1029/2009JD012864.

Boucher, O., D. Randall, P. Artaxo, C. Bretherton, G. Feingold, P. Forster, V.-M. Kerminen, Y. Kondo, H. Liao, U. Lohmann, P. Rasch, S.K. Satheesh, S. Sherwood, B. Stevens and X.Y. Zhang, 2013: Clouds and Aerosols. In: *Climate Change 2013: The Physical Science Basis. Contribution of Working Group I to the Fifth Assessment Report of the Intergovernmental Panel on Climate Change* [Stocker, T.F., D. Qin, G.-K. Plattner, M. Tignor, S.K. Allen, J. Boschung, A. Nauels, Y. Xia, V. Bex and P.M. Midgley (eds.)]. Cambridge University Press, Cambridge, United Kingdom and New York, NY, USA.

Bougiatioti, A., et al. (2014), Processing of biomass burning aerosol in the Eastern Mediterranean during summertime, *Atm. Chem. Phys.*, 14, 4793-4807, doi:10.5194/acp-14-4793-2014.

Canagaratna, M. R., J.L. Jimenez, J. Kroll, Q. Chen, S. Kessler, P. Massoli, L. Hildebrandt Ruiz, E. Fortner, L. Williams, K. Wilson, J. Surratt, N. Donahue, J.T. Jayne, and D.R. Worsnop (2015), Elemental Ratio Measurements of Organic Compounds Using Aerosol Mass Spectrometry: Characterization, Improved Calibration, and Implications, *Atm. Chem. Phys.*, 15, 253-272, doi:10.5194/acp-15-253-2015.

Carrico, C. M., M. H. Bergin, J. Xu, K. Baumann, and H. Maring (2003), Urban aerosol radiative properties: Measurements during the 1999 Atlanta Supersite Experiment, *J. Geophys. Res.* 108(D7), 8422, doi:10.1029/2001JD001222.

Chakrabarty, R. K., H. Moosmuller, L.-W. A. Chen, K. Lewis, W. P. Arnott, C. Massoleni, M. K. Dubey, C. E. Wold, W. M. Hao, and S. M. Kreidenweis (2010), Brown carbon in tar balls from smoldering biomass combustion, *Atm. Chem. Phys.*, *10*, 6363-6370, doi:10.5194/acp-10-6363-2010.

Chen, Y., and T. C. Bond (2010), Light absorption by organic carbon from wood combustion, *Atm. Chem. Phys.*, *10*, 1773-1787, doi:10.5194/acp-10-1773-2010.

Cubison, M. J., Ortega, A. M., Hayes, P. L., Farmer, D. K., Day, D., Lechner, M. J., Brune, W. H., Apel, E., Diskin, G. S., Fisher, J. A., Fuelberg, H. E., Hecobian, A., Knapp, D. J., Mikoviny, T., Riemer, D., Sachse, G. W., Sessions, W., Weber, R. J., Weinheimer, A. J., Wisthaler, A., and Jimenez, J. L. (2011): Effects of aging on organic aerosol from open biomass burning smoke in aircraft and laboratory studies, *Atm. Chem. Phys.*, 11, 12049-12064, doi:10.5194/acp-11-12049-2011.

de Gouw, J. A., et al. (2004), Chemical composition of air masses transported from Asia to the U.S. West Coast during ITCT 2K2: Fossil fuel combustion versus biomass burning signatures, *J. Geophys. Res*., 109, D23S20, doi:10.1029/2003JD004202.

De Haan, D. O. D., Corrigan, A. L., Smith, K. W., Stroik, D. R., Turley, J. J., Lee, F. E., Tolbert, M. A., Jimenez, J. L., Cordova, K. E., and Ferrell, G. R. (2009): Secondary Organic

Aerosol-Forming Reactions of Glyoxal with Amino Acids, *Environ. Sci. Technol*., 43, 2818-2824, 10.1021/es803534f.

DeCarlo, P.F., J.R. Kimmel, A. Trimborn, M.J. Northway, J.T. Jayne, A.C. Aiken, M. Gonin, K. Fuhrer, T. Horvath, K. Docherty, D.R. Worsnop, and J.L. Jimenez, Field-Deployable, High-Resolution, Time-of-Flight Aerosol Mass Spectrometer, *Analytical Chemistry*, 78: 8281-8289, 2006.

Desyaterik, Y., Y. Sun, X. Shen, T. Lee, X. Wang, T. Wang, and J. L. Collett (2013), Speciation of brown carbon in cloud water impacted by agricultural biomass burning in eastern China, *J. Geophys. Res.*, *118*, 7389–7399, doi:7310.1002/jgrd.50561.

Dickerson, R., S. Kondragunta, G. Stenchikov, K. Civerolo, B. Doddridge, and B. Holben (1997), The Impact of Aerosols on Solar Ultraviolet Radiation and Photochemical Smog, *Science*, *278*(5339), 827-830.

Donahue, N., Robinson, A., Trump, E., Riipinen, I., and Kroll, J. (2014): Volatility and Aging of Atmospheric Organic Aerosol, *Topics in Current Chemistry*, 339, 97–143.

Duce, R. A. (1995). Sources, distributions and fluxes of mineral aerosols and their relationship to climate. In R. J. Charlson, & J. Heintzenberg (Eds.), *Aerosol forcing of climate* (pp. 43–72). New York: John Wiley.

Feng, Y., Ramanathan, V., and Kotamarthi, V. R. (2013): Brown carbon: a significant atmospheric absorber of solar radiation?, *Atm. Chem. Phys.*, *13*, 8607-8621, doi:10.5194/acp-13-8607-2013.

Forster, P., Ramaswamy, V., Artaxo, P., Berntsen, T., Betts, R., Fahey, D.W., Haywood, J., Lean, J., Lowe, D.C., Myhre, G., Nganga, J., Prinn, R., Raga, G., Schulz, M., & Van Dorland, R. Miller, H.L. (Ed.). (2007). *Changes in Atmospheric Constituents and in Radiative Forcing Chapter 2*. United Kingdom: Cambridge University Press.

Fuzzi, S., et al (2015), Particulate matter, air quality and climate: lessons learned and future needs, *Atm. Chem. Phys. Disc.*, *15*, 521-744, doi:10.5194/acpd-15-521-2015.

Graber, E. R. and Rudich, Y. (2006): Atmospheric HULIS: How humic-like are they? A comprehensive and critical review*, Atmos. Chem. Phys*., 6, 729-753, doi:10.5194/acp-6-729-2006.

Haywood, J. and K. Shine (1995), The effect of anthropogenic sulfate and soot aerosol on the clear sky planetary radiation budget, *Geophysical Research Letters*, *22*(5), 603-606.

He, S. and G. Carmichael (1999), Sensitivity of photolysis rates and ozone production in the troposphere to aerosol properties, *J. Geophys. Res: Atm*, *104*(D21), 26307-26324.

Hecobian, A., X. Zhang, M. Zheng, N. Frank, E. S. Edgerton, and R. J. Weber (2010), Water-soluble organic aerosol material and the light-absorption characteristics of aqueous extracts measured over the southeastern United States, *Atm. Chem. Phys., 10*, 5965-5977, doi:10.5194/acp-10-5965-2010.

Hennigan, C. J., A. P. Sullivan, J. L. Collett, and A. L. Robinson (2010), Levoglucosan stability in biomass burning particles exposed to hydroxyl radicals, *Geophys. Res. Lett., 37*, L09806, doi:09810.01029/02010GL043088.

Hennigan, C. J., et al. (2011), Chemical and physical transformations of organic aerosol from the photo-oxidation of open biomass burning emissions in an environmental chamber, *Atm. Chem. Phys., 11*, 11995-12037, doi:10.5194/acp-11-7669-2011.

Hobbs, P. V., P. Sinha, R. J. Yokelson, T. J. Christian, D. R. Blake, S. Gao, T. W. Kirchstetter, T. Novakov, and P. Pilewskie, Evolution of gases and particles from a savanna fire in South Africa (2003), *J. Geophys. Res.*, 108(D13), 8485, doi:10.1029/2002JD002352.

Hoffer, A., A. Gelencser, P. Guyon, G. Kiss, O. Schmid, G. P. Frank, P. Artaxo, and M. O. Andreae (2006), Optical properties of humic-like substances (HULIS) in biomass-burning aerosols, *Atm. Chem. Phys., 6*, 3563-3570, doi:10.5194/acp-6-3563-2006.

Iinuma, Y., Böge, O., Gräfe, R., and Herrmann, H. (2010): Methyl Nitrocatechols: Atmospheric tracer compounds for biomass burning secondary organic aerosols, *Environ. Sci. Technol.*, 44, 8453–8459, doi:10.1021/es102938a.

Jacobson, Mark Z. (2001), Strong radiative heating due to the mixing state of black carbon in atmospheric aerosol, *Nature* 409, 695-697, 8 February 2001, doi:10.1038/35055518

Kaufman, Y. J., I. Koren, L. A. Remer, D. Rosenfeld, and Y. Rudich (2005), The effect of smoke, dust and pollution aerosol on shallow cloud development over the Atlantic Ocean, *Proceedings Natl. Acad. Sci*. U.S.A., 102(32), 11,207 – 11,212

Kieber, R. J., R. F. Whitehead, S. N. Reid, J. D. Willey, and P. J. Seaton (2006), Chromophoric dissolved organic matter (CDOM) in rainwater, southeastern North Carolina, USA, *J. Atmos. Chem., 54*, 21-41.

Kirchstetter, T. W., and T. L. Thatcher (2012), Contribution of organic carbon to wood smoke particulate matter absorption of solar radiation, *Atm. Chem. Phys. Disc., 12*, 5803-5816, doi:10.5194/acp-12-6067-2012.

Kitanovski, Z., I. Grgić, F. Yasmeen, M. Claeys, and A. Čusak (2012), Development of a liquid chromatographic method based on ultraviolet–visible and electrospray ionization mass spectrometric detection for the identification of nitrocatechols and related tracers in biomass burning atmospheric organic aerosol, *Rapid Commun. Mass Spectrom.,* 26(7), 793–804, doi:10.1002/RCM.6170.

Lack, D. A., and C. D. Cappa (2010), Impact of brown and clear carbon on light absorption enhancement, single scatter albedo and absorption wavelength dependence of black carbon, *Atm. Chem. Phys., 10*, 4207-4220, doi:10.5194/acp-10-4207-2010.

Lack, D. A., R. Bahreini, J. M. Langridge, J. B. Gilman, and A. M. Middlebrook (2013), Brown carbon absorption linked to organic mass tracers in biomass burning particles, *Atm. Chem. Phys., 13*, 2415-2422, doi:10.5194/acp-13-2415-2013.

Lambe, A. T., Onasch, T. B., Croasdale, D. R., Wright, J. P., Martin, A. T., Franklin, J. P., Massoli, P., Kroll, J. H., Canagaratna, M. R., Brune, W. H., Worsnop, D. R., and Davidovits, P. (2012): Transitions from Functionalization to Fragmentation Reactions of Laboratory Secondary Organic Aerosol (SOA) Generated from the OH Oxidation of Alkane Precursors, *Environ. Sci. Technol.*, 46, 5430–5437, doi:10.1021/es300274t.

Laskin, Julia, Alexander Laskin, Sergey A. Nizkorodov, Patrick Roach, Peter Eckert, Mary K. Gilles, Bingbing Wang, Hyun Ji (Julie) Lee, Qichi Hu, Molecular Selectivity of Brown Carbon Chromophores (2014), *Environ. Sci. Technol.*, 48, 20, 12047, doi: 10.1021/es503432r.

Laskin, A., Laskin, J., and Nizkorodov, S. A.: Chemistry of Atmospheric Brown Carbon, *Chem. Rev*., 115, 4335–4382, doi:10.1021/cr5006167, 2015.

Lee, H. J., P. K. Aiona, A. Laskin, J. Laskin, and S. A. Nizkorodov (2014), Effect of Solar Radiation on the Optical Properties and Molecular Composition of Laboratory Proxies of Atmospheric Brown Carbon, *Environ. Sci. Technol*, *48*, 10217-10226, doi: 10.1021/es502515r.

Limbeck, A., Kulmala, M., and Puxbaum, H. (2003): Secondary organic aerosol formation in the atmosphere via heterogeneous reaction of gaseous isoprene on acidic particles, *Geophysical Research Letters*, 30, 1996, 10.1029/2003GL017738.

Lin, G., Penner, J. E., Flanner, M. G., Sillman, S., Xu, L., and Zhou, C.: Radiative forcing of organic aerosol in the atmosphere and on snow: Effects of SOA and brown carbon, J. *Geophys. Res. Atmos*., 119, 7453–7476, 2014.

Lin, P., Laskin, J., Nizkorodov, S. A., and Laskin, A. (2015): Revealing Brown Carbon Chromophores Produced in 586 Reactions of Methylglyoxal with Ammonium Sulfate, *Environ Sci Technol*, 49 (24), 14257–14266, 587 10.1021/acs.est.5b03608

Liu, J., Bergin, M., Guo, H., King, L., Kotra, N., Edgerton, E., and Weber, R. J.: Size-resolved measurements of brown carbon in water and methanol extracts and estimates of their contribution to ambient fine-particle light absorption, *Atmos. Chem. Phys.*, 13, 12389-12404, doi:10.5194/acp-13-12389-2013, 2013.

Liu, J., et al. (2014), Brown carbon in the continential troposphere, *Geophys. Res. Lett., 41*, 2191–2195, doi:2110.1002/2013GL058976.

Liu, J., W. Scheuer, J. Dibb, G. Diskin, L. Ziemba, K. L. Thornhill, B. Anderson, A. Wisthaler, T. Mikoviny, J. Jaidevi, M. Bergin, A. Perring, M. Markovic, J. Schwarz, P. Campuzano-Jost, D. Day, J. L. Jimenez, and R. J. Weber (2015), Brown Carbon Aerosol in the North American Continental Troposphere: Sources, Abundance, and Radiative Forcing, *Atmos. Chem. Phys. Disc.*, *15*, 5959-6007.

Lu, Z., D. G. Streets, E. Winijkul, F. Yan, Y. Chen, T. C. Bond, Y. Feng, M. K. Dubey, S. Liu, J. P. Pinto, and G. R. Carmichael (2015), Light absorption properties and radiative effects of primary organic aerosol emissions, *Environ. Sci. Technol.*, 49, 4868-4877.

McNaughton, C., et al. (2007), Results from the DC-8 inlet characterization experiment (DICE): Airborne versus surface sampling of mineral dust and sea salt aerosols, *Aerosol Sci. Technol.*, 41, 136–159.

Molina, M. J., Ivanov, A. V., Trakhtenberg, S., and Molina, L. T. (2004): Atmospheric evolution of organic aerosol, *Geophys. Res. Lett*., 31, L22104, doi:10.1029/2004gl020910.

Nakayama, T., K. Sato, Y. Matsumi, T. Imamura, A. Yamazaki, and A. Uchiyama (2013), Wavelength and NOx dependent complex refractive index of SOAs generated from the photooxidation of toluene, *Atm. Chem. Phys.*, *13*, 531-545, doi:10.5194/acp-13-531-2013.

Nguyen, T. B., P. B. Lee, K. M. Updyke, D. L. Bones, J. Laskin, A. Laskin, and S. A. Nizkorodov (2012), Formation of nitrogen- and sulfur-containing light-absorbing compounds accelerated by evaporation of water from secondary organic aerosols, *J. Geophys. Res*., 117, D01207, doi:10.1029/2011JD016944.

Park, R. J., Kim, M. J., Jeong, J. I., Youn, D., and Kim, S.: A contribution of brown carbon aerosol to the aerosol light absorption and its radiative forcing in East Asia, *Atmos. Environ*., 44, 1414–1421, 2010.

Perry, K. D., S. S. Cliff, and M. P. Jimenez-Cruz (2004), Evidence for hygroscopic mineral dust particles from the Intercontinental Transport and Chemical Transformation Experiment, *J. Geophys. Res*., 109, D23S28, doi:10.1029/2004JD004979.

Petzold, A., Rasp, K., Weinzierl, B., Esselborn, M., Hamburger, T., Dornbrack, A., Kandler, K., Schutz, L., Knippertz, P., Fiebig, M., and Virkkula, A. (2009), Saharan dust absorption and refractive index from aircraft-based observations during SAMUM 2006. *Tellus B*, 61: 118–130. doi:10.1111/j.1600-0889.2008.00383.x

Reid, J.S. and Hobbs, P.V. (1998). Physical and optical properties of young smoke from individual biomass fires in Brazil. *Journal of Geophysical Research 103: doi: 10.1029/98JD00159. issn: 0148-0227.*

Ricchiazzi, P., S. Yang, C. Gautier, and D. Sowle (1998), SBDART, A research and teaching tool for plane-parellel radiative transfer in the Earth's atmosphere, Bull. *Am. Meteorol. Soc.*, 79, 2101– 211.

Robinson, A. L., Donahue, N. M., Shrivastava, M. K., Weitkamp, E. A., Sage, A. M., Grieshop, A. P., Lane, T. E., Pierce, J. R., and Pandis, S. N. (2007): Rethinking Organic Aerosols: Semivolatile Emissions and Photochemical Aging, *Science*, 315, 1259–1262, doi:10.1126/science.1133061.

Sachse, G. W., G. F. Hill, L. O. Wade, and M. G. Perry (1987), Fast-response, high-precision carbon monoxide sensor using a tunable diode laser absorption technique, *J. Geophys. Res.*, *92*, 2071-2081, doi:10.1029/JD092iD02p02071.

Saleh, R., Hennigan, C. J., McMeeking, G. R., Chuang, W. K., Robinson, E. S., Coe, H., Donahue, N. M., and Robinson, A. L. (2013): Absorptivity of brown carbon in fresh and photo-chemically aged biomass-burning emissions, *Atmos. Chem. Phys.*, 13, 7683–7693, doi:10.5194/acp-13-7683-2013.

Saleh, R., E. S. Robinson, D. S. Tkacik, A. T Ahern, S. Liu, A. C. Aiken, R. C. Sullivan, A. A Presto, M. K. Dubey, R. J. Yokelson, N. M. Donahue, A. L. Robinson (2014), Brownness of organics in aerosols from biomass burning linked to their black carbon content, *Nature Geoscience*, 7, 647-650, doi: 10.1038/NGEO2220.

Saleh, R., M. Marks, J. Heo, P. J. Adams, N. M. Donahue, and A. L. Robinson (2015), Contribution of brown carbon and lensing to the direct radiative effect of carbonaceous aerosols from biomass and biofuel burning emissions, *J. Geophys. Res. Atmos.*, 120, 10,285–10,296, doi:10.1002/2015JD023697.

Sareen, N., A. N. Schwier, E. L. Shapiro, D. Mitroo, and V. F. McNeil (2010), Secondary organic material formed by methylglyoxal in aqueous aerosol mimics, *Atm. Chem. Phys.* , *10*, 997-1016, doi:10.5194/acp-10-997-2010.

Schnaiter, M., Linke, C., Mohler, O., Naumann, K.H., Saathoff, H., Wagner, R., € Schurath, U., Wehner, B., 2005. Absorption amplification of black carbon internally mixed with secondary organic aerosol. *J. Geophy. Res. Atmos.* 110, D19204.

Schuster, G., O. Dubovik, and A. Arola (2016a), Remote sensing of soot carbon – Part 1: Distinguishing different absorbing aerosol species, *Atmospheric Chemistry and Physics*, *16*(3), 1565-1585.

Schuster, G., O. Dubovik, A. Arola, T. Eck, and B. Holben (2016b), Remote sensing of soot carbon– Part 2: Understanding the absorption Ångström exponent, *Atmospheric Chemistry and Physics*, *16*(3), 1587-1602.

Schwarz, J. P., J. R. Spackman, D. W. Fahey, R. S. Gao, U. Lohmann, P. Stier, L. A. Watts, D. S. Thomson, D. A. Lack, L. Pfister, M. J. Mahoney, D. Baumgardner, J. C. Wilson, and J.

M. Reeves (2008), Coatings and their enhancement of black carbon light absorption in the tropical atmosphere, *J. Geophys. Res.*, *113*, D03203, doi:03210.01029/02007JD009042.

Shapiro, E. L., J. Szprengiel, N. Sareen, C. N. Jen, M. R. Giordano, and V. F. McNeill (2009), Light-absorbing secondary organic material formed by glyoxal in aqueous aerosol mimics, *Atm. Chem. Phys.*, *9*, 2289-2300, doi:10.5194/acp-9-2289-2009.

Sokolik, I., and O. Toon (1999), Incorporation of mineralogical composition into models of the radiative properties of mineral aerosol from UV to IR wavelengths, *J. Geophys. Res*., 104, 9423–9444, doi:10.1029/1998JD200048.

Spracklen, D., J. Logan, L. Mickley, R. Park, R. Yevich, A. Westerling, and D. Jaffe (2007), Wildfires drive interannual variability of organic carbon aerosol in the western U.S. in summer, *Geophys. Res. Lett.*, 34, L16816, doi:10.1029/2007GL030037.

Sun, H., Biedermann, L., and Bond, T. C.: The color of brown carbon: A model for ultraviolet and visible light absorption by organic carbon aerosol, *Geophys. Res. Lett.*, 34, L17813, doi:10.1029/2007GL029797, 2007.

Toon, O. B., et al. (2016), Planning, implementation, and scientific goals of the Studies of Emissions and Atmospheric Composition, Clouds and Climate Coupling by Regional Surveys (SEAC4RS) field mission, *J. Geophys. Res. Atmos.*, 121, 4967–5009, doi:10.1002/2015JD024297.

U.S. EPA. 2013 Final Report: Integrated Science Assessment of Ozone and Related Photochemical Oxidants. U.S. Environmental Protection Agency, Washington, DC, EPA/600/R-10/076F, 2013.

Virkkula, A. (2010): Correction of the calibration of the 3-wavelength Particle Soot Absorption Photometer (3λPSAP), *Aerosol Sci. Tech.*, 44:8, 706-712, doi: 10.1080/02786826.2010.482110

Washenfelder, R. A., A. R. Attwood, C. A. Brock, H. Guo, L. Xu, R. J. Weber, N. L. Ng, H. M. Allen, W. R. Ayres, K. Baumann, R. C. Cohen, D. C. Draper, K. C. Duffey, E. Edgerton, J. L. Fry, W. W. Hu, J. L. Jimenez, B. B. Palm, P. Romer, E. A. Stone, P. J. Wooldridge, and S. S. Brown (2015), Biomass burning dominates brown carbon absorption in the rural southeastern United States, *Geophys. Res. Lett.*, doi:10.1002/2014GL062444.

Yokelson, R., R. Susott, D. E. Ward, J. Reardon, D. W. T. Griffith (1997), Emissions from smoldering combustion of biomass measured by open-path Fourier transform infrared spectroscopy, J. Geophys. Res., 102, No. D15, 18865-18877.

Zarzana, K. J., D. O. D. Haan, M. A. Freedman, C. A. Hasenkopf, and M. A. Tolbert (2012), Optical Properties of the Products of α-Dicarbonyl and Amine Reactions in Simulated Cloud Droplets, *Environ. Sci. Technol.*, *46*(9), 4845-4851, doi:10.1021/es2040152.

Zhang, X.; Lin, Y,-H.; Surratt, J. D.; Zotter, P.; Prevó ̂t, A. H. S.; Weber, R. J. (2011), Light-absorbing soluble organic aerosol in Los Angeles and Atlanta: A contrast in secondary organic aerosol. *Geophys. Res. Lett*. 2011, 38, L21810 DOI: 10.1029/2011GL049385.

Zhang, X., Y.-H. Lin, J. D. Surratt, and R. J. Weber (2013), Sources, composition and absorption angström exponent of light-absorbing organic components in aerosol extracts from the Los Angeles Basin, *Environ. Sci. Technol*., 47(8), 3685–3693.

Zhang, Y., et al. (2017), Top-of-atmosphere radiative forcing affected by brown carbon in the upper troposphere, *Nature Geoscience* 10, 486-489 (2017).

Zhao, R., A. K. Y. Lee, L. Huang, X. Li, F. Yang, and J. P. D. Abbatt (2015), Photochemical Processing of Aqueous Atmospheric Brown Carbon, *Atm. Chem. Phys. Disc.*, doi:10.5194/acpd-15-2957-2015.

Zhong, M., and M. Jang (2014), Dynamic light absorption of biomass burning organic carbon photochemically aged under natural sunlight, *Atm. Chem. Phys.*, *14*, 1517-1525, doi:10.5194/acp-14-1517-2014